Broad geographic sampling reveals predictable, pervasive, and strong seasonal adaptation in *Drosophila*

Heather E. Machado[1,2*‡], Alan O. Bergland[1,3*‡], Ryan Taylor[1], Susanne Tilk[1], Emily Behrman[4], Kelly Dyer[5], Daniel K. Fabian[6,7], Thomas Flatt[6,8], Josefa González[9], Talia L. Karasov[10], Bernard Kim[1], Iryna Kozeretska[11,12], Brian P. Lazzaro[13], Thomas JS Merritt[14], John E. Pool[15], Katherine O'Brien[4], Subhash Rajpurohit[4], Paula R. Roy[16], Stephen W. Schaeffer[17], Svitlana Serga[11,12], Paul Schmidt[4°‡], Dmitri A. Petrov[1°‡]

* equal contribution
° equal contribution
‡ to whom correspondence should be addressed: heather.machado@sanger.ac.uk, aob2x@virginia.edu, schmidtp@upenn.edu, dpetrov@stanford.edu

[1] Department of Biology, Stanford University, Stanford, CA, United States
[2] Wellcome Sanger Institute, Hinxton CB10 1SA, United Kingdom
[3] Department of Biology, University of Virginia, Charlottesville, VA, United States
[4] Department of Biology, University of Pennsylvania, Philadelphia, PA, United States
[5] Department of Genetics, University of Georgia, Athens, GA, United States
[6] Institute of Population Genetics, Vetmeduni Vienna, A-1210 Vienna, Austria
[7] Centre for Pathogen Evolution, Department of Zoology, University of Cambridge, Cambridge CB2 3EJ, United Kingdom
[8] Department of Biology, University of Fribourg, CH-1700 Fribourg, Switzerland
[9] Institute of Evolutionary Biology, CSIC- Universitat Pompeu Fabra, Barcelona, Spain
[10] Department of Biology, University of Utah, Salt Lake City, UT, United States
[11] Taras Shevchenko National University of Kyiv, Kyiv, Ukraine
[12] National Antarctic Scientific Centre of Ukraine, Taras Shevchenko Blvd., 01601, Kyiv, Ukraine
[13] Department of Entomology, Cornell University, Ithaca, NY, United States
[14] Department of Chemistry & Biochemistry, Laurentian University, Sudbury, ON, Canada
[15] Laboratory of Genetics, University of Wisconsin-Madison, Madison, WI, United States
[16] Department of Ecology and Evolutionary Biology, University of Kansas, Lawrence, KS, United States
[17] Department of Biology, The Pennsylvania State University, University Park, PA, United States

Abstract

To advance our understanding of adaptation to temporally varying selection pressures, we identified signatures of seasonal adaptation occurring in parallel among *Drosophila melanogaster* populations. Specifically, we estimated allele frequencies genome-wide from flies sampled early and late in the growing season from 20 widely dispersed populations. We identified parallel seasonal allele frequency shifts across North America and Europe, demonstrating that seasonal adaptation is a general phenomenon of temperate fly populations. Seasonally fluctuating polymorphisms are enriched in large chromosomal inversions and we find a broad concordance between seasonal and spatial allele frequency change. The direction of allele frequency change at seasonally variable polymorphisms can be predicted by weather conditions in the weeks prior to sampling, linking the environment and the genomic response to selection. Our results suggest that fluctuating selection is an important evolutionary force affecting patterns of genetic variation in *Drosophila*.

Introduction

Fluctuations in the environment are an inescapable condition for all organisms. While many of these fluctuations are entirely unpredictable, some are predictable to a degree, including those that occur on diurnal and seasonal time scales. The predictability of cyclic fluctuations is reflected in the fact that many species exhibit plastic physiological and behavioral strategies that enable them to survive the unfavorable season and exploit the favorable one (Denlinger, 2002; Kostál, 2006); such plastic responses represent the classical form of seasonal adaptation (Tauber et al., 1986). However, seasonally varying selection can - in principle - maintain fitness-related genetic variation if some genotypes have high fitness in one season but not another (Gillespie, 1973; Haldane and Jayakar, 1963). Thus, in organisms that undergo multiple generations per year, a distinct form of seasonal adaptation occurs when the frequency of alternate genotypes changes in response to seasonal fluctuations in the environment.

Seasonal adaptation can be seen as a form of local adaptation- local adaptation in time to temporally varying selection pressures rather than in space. Such adaptation in time has often been considered to be uncommon and, when present, unlikely to result in long-term balancing selection (Ewing, 1979; Hedrick, 1976). Classic quantitative genetic theory suggests that an optimal, plastic genotype will eventually dominate a population that is exposed to periodically changing environments (Bürger and Gimelfarb, 1999; Korol et al., 1996; Lande, 2008; Scheiner, 1993). This is particularly so when certain environmental cues are reliable indicators of changes in selection pressure (Levins, 1974; Via and Lande, 1985). Predictions from traditional population genetic models suggest that periodically changing environments will lead to the rapid loss of seasonally favored ecotypes as slight changes in selection pressure from one year to another eventually push allele frequencies at causal alleles to fixation (Hedrick, 1976).

Recent theoretical models have called these classical predictions into question. For instance, a quantitative genetic model by Botero and colleagues (Botero et al., 2015) examined whether adaptive tracking, plasticity, or bet-hedging evolve as a consequence of environmental fluctuations. They showed that adaptive tracking rather than plasticity is likely to become a predominant feature of populations living in seasonally fluctuating environments when populations undergo more than three generations per season. Additionally, a population genetic model by Wittmann and colleagues (Wittmann et al., 2017) has demonstrated that seasonally varying selection can indeed maintain fitness related genetic variation at many loci throughout the genome provided that dominance shifts from season to season in such a way that, on average, the seasonally favored allele remains slightly dominant (Curtsinger et al., 1994). These recent models, along with others that highlight the importance of population cycles (Bertram and Masel, 2019), as well as overlapping generations and age structure (Bertram and Masel, 2019; Ellner, 1996; Ellner and Hairston, 1994; Ellner and Sasaki, 1996), suggest that seasonal adaptation and adaptive tracking (Kain et al., 2015) could be an important feature of organisms such as *Drosophila* that have multiple generations per year (Behrman et al., 2015). More generally, it is possible that adaptive tracking of environmental fluctuations on rapid time scales might be more common than generally acknowledged and has been hidden from us

due to the difficulty of detecting such adaptive tracking reliably (Lynch and Ho, 2020) and from the lack of finely resolved temporal data (Buffalo and Coop, 2020).

Despite the lack of theoretical consensus on whether and how seasonal adaptation operates, there is substantial empirical evidence for seasonal adaptation in many organisms including *Drosophila*. Seasonal adaptation was first observed in *D. pseudoobscura* by Dobzhansky and colleagues (e.g., Dobzhansky, 1943) by tracking frequencies of inversion polymorphisms over seasons. Later studies confirmed and extended these early findings to other species including *D. melanogaster* (Kapun et al., 2016; Stalker, 1980, 1976) and *D. subobscura* (Rodríguez-Trelles et al., 2013).

In *D. melanogaster*, multiple additional lines of evidence from phenotypic and genetic analyses demonstrate the presence of seasonal adaptation. When reared in a common laboratory environment, flies collected in winter or spring (close descendants of flies that successfully overwintered) show higher stress tolerance (Behrman et al., 2015), greater propensity to enter reproductive dormancy (Schmidt and Conde, 2006), increased innate immune function (Behrman et al., 2018), and modulated cuticular hydrocarbon profiles (Rajpurohit et al., 2017) as compared to flies collected in the fall (the descendants of those flies who prospered during the summer). Rapid adaptation over seasonal time scales in these and related phenotypes has also been observed in laboratory (Schmidt and Conde, 2006) and field-based mesocosm experiments (Erickson et al., 2020; Grainger et al. 2021; Rajpurohit et al., 2018, 2017; Rudman et al., 2019). Genome-wide analysis indicated that a large number of common polymorphisms change in frequency over seasonal time scales in one mid-latitude orchard (Bergland et al., 2014), and allele frequency change among seasons has been observed using candidate gene approaches (Cogni et al., 2014). In several cases, these adaptively oscillating polymorphisms have been linked to seasonally varying phenotypes (Behrman et al., 2018; Erickson et al., 2020; Paaby et al., 2014).

Despite ample evidence of seasonal adaptation in *D. melanogaster*, many aspects of this system remain unexplored. First, we do not know whether seasonal adaptation is a general feature of *D.*

82 *melanogaster* populations across its range. Previous work (Schmidt and Conde 2006, Bergland et al.
83 2014, Cogni et al. 2014, Behrman et al. 2015, Behrman et al. 2018) detected seasonal allele frequency
84 fluctuations in a single locality over the span of one to three years. These results need to be confirmed
85 at other locations. Second, as many ecological and environmental variables covary with season, it is
86 unclear which specific factors drive the observed changes in phenotype and genotype in populations
87 sampled over seasonal time. One straightforward and statistically powerful way to start answering
88 these questions is to assess the extent of parallel shifts in allele frequencies over seasonal time in
89 many populations across the *D. melanogaster* range. Should such parallel shifts be detected we can
90 then infer that seasonal adaptation is widespread and at least partly driven by a common set of
91 variants. We can also attempt to associate the magnitude and direction of allelic shifts with local
92 environmental conditions (e.g., temperature) that may vary among populations sampled at equivalent
93 points in seasonal time. Broad sampling will also allow us to determine the magnitude of the shared
94 seasonal fluctuations and give us a glimpse into the genetic architecture of seasonal adaptation: for
95 instance, whether or not the seasonally-responsive variants are found genome-wide or clustered into
96 linked blocks or even supergenes.
97
98 Here we carry out such a study by using allele frequency data from 20 paired seasonal samples from
99 15 localities in North America and Europe. First, we demonstrate that seasonal adaptation is a general
100 phenomenon that occurs in multiple populations of *D. melanogaster* on two continents by providing
101 evidence that at least some of the same polymorphisms cycle between seasons in populations sampled
102 across vast geographic distances. Seasonal alleles tend to show clinal variation, with the alleles that
103 increase in frequency through the summer generally being more frequent in lower latitude (more
104 "summer-like") locations. We also show that seasonal signal is enriched near inversion breakpoints or
105 within inverted regions on chromosome 2L, 3L, and 3R, although these inverted regions do not
106 account for all of the signal that we observe. Further, we show that allele frequency change between
107 seasons is most predictable when taking into account the local temperature prior to sample collections
108 both in the spring and in the fall, which hints at the complex and nonlinear nature of adaptation with
109 adaptive tracking occurring at sub-seasonal timescales. Taken together, our work demonstrates that

110 seasonal adaptation is a general and predictable feature of *D. melanogaster* populations and has
111 pervasive effects on patterns of allele frequencies genome-wide. More generally we establish that
112 metazoan populations can exhibit polygenic adaptive tracking of environmental conditions on
113 extremely short time scales, most likely shorter than a single growing season encompassing ~10
114 generations.
115

116 ## ***Results***

117 **Fly samples and sequence data**

118 We assembled 73 samples of *D. melanogaster* collected from 23 localities in North America and
119 Europe (Supplemental Table 1, Supplemental Figure 1). For 15 sampling localities, flies were
120 collected in the spring and fall over the course of one to six years (Figure 1A). Our sampling and
121 sequencing efforts also complement other genome-wide datasets that investigate genetic variation
122 within and among *D. melanogaster* populations throughout their range (Campo et al., 2013; Fabian et
123 al., 2012; Grenier et al., 2015; Kao et al., 2015; Kapun et al., 2020; Kim et al., 2014; Kolaczkowski et
124 al., 2011; Lack et al., 2016; Mackay et al., 2012; Pool et al., 2012; Reinhardt et al., 2014; Svetec et al.,
125 2016; Zhao and Begun, 2017).
126

127 For our analysis, we divided our samples into two subsets (Figure 1B). The first subset ('Core20') is
128 composed of 20 pairs of spring and fall samples from the same location. Samples in the Core20 set
129 are drawn from 15 localities in North America and Europe and we use at most two years of sampling
130 from any one locality. The second subset of samples ('Clinal') was used to examine patterns of clinal
131 variation along the East Coast of North America and consists of four populations sampled in the
132 spring (see Material and Methods and Supplemental Table 1).
133

134 To estimate allele frequencies genome-wide we performed pooled DNA sequencing of multiple
135 individual flies per population (Schlötterer et al., 2014; Zhu et al., 2012). For each sample, we
136 resequenced pools of ~75 individuals (range 27-164) to an average of 94x coverage (range 22-220,

Supplemental Table 1). Analyses presented here use a total of 43 samples in the Core20 and Clinal sets described above. Data from the remaining 30 samples, including those that do not constitute paired spring/fall samples, are not included in our analyses here but nonetheless form a part of our larger community-based sampling and resequencing effort and are deposited with the rest of the data (NCBI SRA; BioProject Accession #PRJNA308584; accession numbers for each sample can be found in Supplemental Table 1).

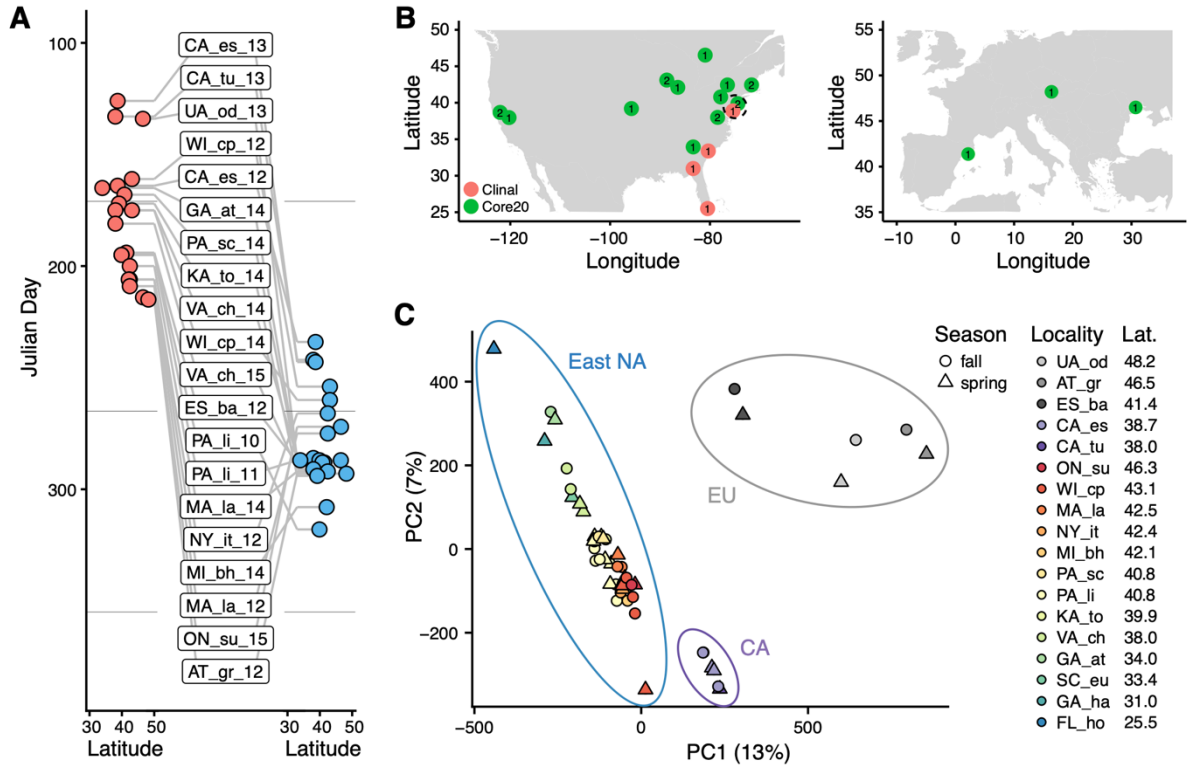

Figure 1. Sampling times, localities, and basic population structure of samples used in this study. (A) Distribution of collection times during the spring (red) and fall (blue) in relation to latitude. For samples where the collection month, but not day, was recorded, we specified the 15th of the month to calculate Julian Day. (B) Sampling localities for the primary seasonal analysis ('Core20': green) and the latitudinal cline analysis ('Cline': red), distributed across North America and Europe. Numbers represent the number of years of spring/fall comparisons at that locality. (C) Principal components analysis of SNP allele frequencies. Circles are placed around samples from three geographic regions: Europe (EU), California (CA) and Eastern North America (East NA); points are colored by latitude and shapes represent seasons, as defined by collection time.

Pooled resequencing identified ~1.75M SNPs following quality control and filtering for read depth and average minor allele frequency (minor allele frequency > 0.01). We applied a second filtering and retained ~775,000 SNPs that have observed polymorphism in each population sampled. This biases us towards assessing fluctuations at higher frequency polymorphisms (Supplemental Figure 2). Because

149 this dataset represents approximately half of all detected SNPs, the conclusions drawn from its
150 analysis are representative of genetic variation in *D. melanogaster*.
151
152 To gain insight into basic patterns of differentiation among the sampled populations, we performed a
153 principal component (PC) analysis across all samples. Samples cluster by locality and geography
154 (Figure 1C) with PC 1 separating European, North American West Coast and East Coast populations
155 while PC 2 separates the eastern North America samples by latitude (linear regression $p = 3*10^{-15}$, R^2
156 = 0.84). No PC is associated with season, following correction for multiple testing, implying that the
157 spatial differentiation dominates patterns of SNP variation across these samples.
158
159 **Seasonal adaptation is a general feature of *D. melanogaster* populations**
160 Our first objective was to determine whether or not we find evidence of parallel seasonal cycling of
161 allele frequencies across multiple populations. To identify a signal of parallel allele frequency change
162 over time we assessed the per-SNP change in allele frequency between spring and fall among the
163 Core20 set of populations using three complementary methods that rely on different statistical models.
164 For all three methods, we contrast the observed signal to permutations in which we shuffled the
165 seasonal labels within each spring-fall paired sample. With the exception of the seasonal labels within
166 paired samples, these permutations have the advantage of retaining all of the features of the data
167 including patterns of genetic covariation and all of the noise in the allele frequency estimation.
168
169 We first used a generalized linear model (GLM), regressing allele frequency at each SNP on season
170 across all of the populations. We find that the observed genome-wide distribution of 'seasonal' *p*-
171 values from this model is not uniform and there is a pronounced excess of SNPs with low *p*-values
172 (Figure 2A). The observed data have a stronger seasonal signal than most permutations. For example,
173 at a *p*-value of $\sim 4*10^{-3}$, which corresponds to the top 1% (Supplemental Table 2), the observed data
174 have a greater number of seasonal SNPs than 96.8% of the permutations (Figure 2B). This enrichment
175 is robust to the choice of quantile (Supplemental Figure 4). Seasonal SNPs identified by Bergland and
176 colleagues (2014) are slightly enriched among the top 1% of SNPs identified using the GLM, relative

177 to matched genomic controls, after excluding the overlapping Pennsylvanian populations ($\log_2$ odds

178 ratio ± SD = 0.59 ± 0.37, p_{perm} = 0.0512). Our top set of seasonally variable SNPs shift in frequency

179 by ~4-8% (Fig. 2C). Taken at face value this corresponds to effective selection coefficients of ~10-

180 30% per season (~1-3% per generation assuming 10 generations per season).

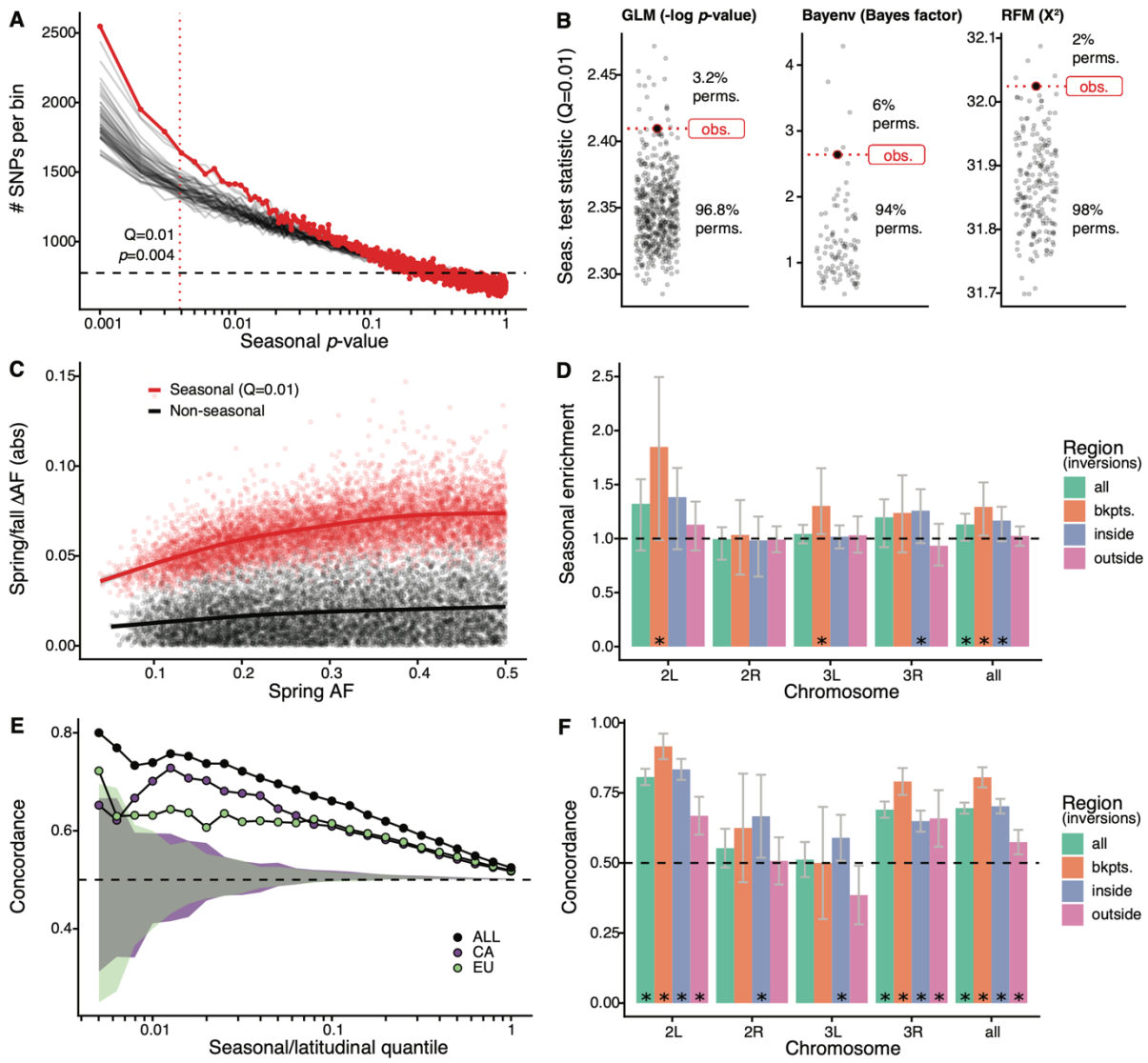

181

Figure 2. **Signals of seasonal adaptation.** (A) *P*-value distribution of GLM seasonal regression (red line), permutations (solid black lines, 50/500 plotted), and expected values (dashed black line). (B) Comparison of seasonal test statistics (quantile=0.01) for observed (red) and permuted (black) datasets, for the three analyses: i: GLM (-log p-value), ii: Bayenv (Bayes factor; outlier of a Bayes factor of 10 excluded from plotting), iii: RFM (X^2). (C) Average spring/fall allele frequency change for each of the top 1% of seasonally varying SNPs (red) and non-seasonal, matched control SNPs (black), as a function of the folded spring allele frequency. Lines represent a moving average across SNPs with a given spring allele frequency. (D) Enrichment of seasonal SNPs (median of 500 permutations). Enrichment is calculated as the observed number of seasonal SNPs over the number of seasonal SNPs in each permutation at P<0.004. The genome is subset by chromosome and location relative to major cosmopolitan inversions (bkpts.: inversion breakpoints +/- 1Mb, inside: interior to the breakpoints excluding 1Mb buffer, outside: exterior to the breakpoints excluding the 1Mb

buffers). Error bars are 95% confidence intervals and asterisks denote greater seasonal enrichment than more than 95% of permutations. (E/F) Concordance rates of seasonal and clinal polymorphisms by E) geographic region and F) genomic region. The y-axis represents the concordance rate of allele frequency change across time and space, assuming that the winter favored allele is the same as the allele favored in high latitudes. Clinal polymorphisms were identified along the East Coast of North America. Seasonal sites were identified using all populations not used in the clinal analysis (n=18). E) Seasonal sites were also identified using exclusively the California populations (purple: n=3) or the Europe populations (green: n=3). Shaded areas are the 95% confidence intervals of 100 matched control datasets for the Californian (purple) and European (green) analyses. F) Concordance by genomic region. Error bars are 95% confidence intervals (binomial error) and asterisks denote concordance significantly greater than 0.5 (binomial test $p<0.05$).

Next, we performed a parallel analysis using a Bayesian model, Bayenv, which uses a population covariance matrix to account for structure among samples (Günther and Coop, 2013). We found an enrichment of seasonal SNPs at high test statistic values (quantile = 0.01: Bayes factor = 2.6), with a greater enrichment of seasonal SNPs compared with 94% of permutations (Figure 2B). The set of seasonal SNPs identified in the Bayenv analysis shows substantial overlap with the GLM set. Specifically, for the top 1% of SNPs in the GLM analysis, 20% are also in the top 1% of the Bayenv analysis, compared with a naive expectation of 1% (Supplemental Figure 4).

Finally, we developed a method derived from combining ranked-normalized *p*-values from Fisher's Exact Tests that compares allele frequencies within each pair of seasonal samples (see Materials and Methods). We again find a deviation from the expected test statistic distribution indicating an excess of seasonally varying polymorphisms (Figure 2B) with the observed enrichment of high scores (quantile = 0.01: $X^2 = 32$) to be greater than more than 98% of permutations. These three analyses, using entirely distinct statistical machinery and assumptions, together provide strong evidence of the genome-wide excess of seasonal SNPs indicating a robust signal of parallel seasonal adaptation across multiple populations.

We examined whether seasonally variable SNPs are enriched on any particular chromosome. To perform this test, we calculated the enrichment of seasonal SNPs per chromosome in the observed data relative to the permutations (Figure 2D). Chromosomes 2L and 3R have the greatest nominal enrichment of seasonal SNPs relative to permutations, with a mean increase of 30% ($p = 0.06$) and of

204 18% (p = 0.08), respectively. Enrichment is much lower for chromosomes 2R and 3L (-2% and 4%, p
205 = 0.54 and p = 0.20, respectively). The variation of the seasonal signal across chromosomes is
206 statistically significant (ANOVA, $p < 10^{-15}$).
207
208 As chromosomal inversions have been observed to fluctuate in frequency over seasonal time
209 (Dobzhansky, 1948, 1943; Kapun et al., 2016), we extended the analysis to focus on large
210 cosmopolitan inversions. We find that regions near inversion breakpoints (± 0.5Mb) on chromosomes
211 2L (p = 0.03, inversion *In(2L)t*) and 3L (p = 0.01, inversion *In(3L)Payne*) are enriched for seasonal
212 SNPs. Regions within the three inversions on chromosome 3R (*In(3R)Mo*, *In(3R)K*, *In(3R)Payne*) are
213 also enriched for seasonal SNPs (p = 0.05). We do not find evidence for enrichment of seasonal SNPs
214 associated with *In(2R)NS* as previously reported by Kapun et al. (2016). These data confirm that
215 inversions may play a role in the adaptive response to seasonally variable environments, similar to
216 that of structural variants or large haplotype blocks in other systems (Hager et al., 2021; Jones et al.,
217 2012; Samuk et al., 2017; Tuttle et al., 2016).
218
219 **Latitudinal differentiation parallels signatures of seasonal adaptation**
220 Parallel changes in phenotype and genotype across time and space have been observed in *D.*
221 *melanogaster* (Bergland et al., 2014; Cogni et al., 2015, 2014; Kapun et al., 2016; Kapun and Flatt,
222 2019; Paaby et al., 2014; Rajpurohit et al., 2018, 2017). To assess whether we observe similar patterns
223 in our data, we tested whether SNPs that change in allele frequency along a latitudinal cline and
224 across seasons do so in a parallel fashion. Parallel changes in allele frequency occur when the sign of
225 the allele frequency change between spring and fall is the same as between high- and low-latitude
226 populations. Using four populations along the East Coast latitudinal cline, we identified clinally
227 varying polymorphisms using single-locus models (GLM, with allele frequency regressed against
228 latitude) as well as a model that accounts for population structure (Bayenv; Günther and Coop, 2013).
229 We re-identified seasonally varying SNPs using a GLM (as done previously) using 18 of the Core20
230 populations to avoid two samples drawn from a shared collection locale with the clinal set (PA_li;
231 Supplemental Table 1).

232

233 We find significant seasonal and latitudinal parallelism, with the magnitude of parallelism increasing
234 with increasing GLM significance thresholds (Figure 2E). Among the polymorphisms that are in the
235 top 1% of both seasonal and clinal GLMs (n = 115), 74% have parallel allele frequency change
236 (greater than 100/100 matched controls; naive expectation: 50%). This pattern of parallelism is also
237 observed when using a Bayenv model of clinality (Supplemental Figure 5). Parallel changes in allele
238 frequency between seasons and clines that we observe here is similar to previously published genome-
239 wide (Bergland et al., 2014) and locus specific results (Cogni et al., 2014; Kapun et al., 2016; Stalker,
240 1980, 1976, p. 197).

241

242 To evaluate whether parallel allele frequency change across time and space are likely to be
243 independent of shared demographic processes such as local seasonal migration, we compared East
244 Coast clinal variation to seasonal variation identified in two groups of populations that are
245 geographically and genetically distant from the East Coast (Campo et al., 2013; and see Figure 1B)
246 and that are unlikely to be connected via common seasonal migration. We assessed seasonal changes
247 in allele frequency separately for Californian (n = 3) and European (n = 3) populations and tested for
248 parallelism with polymorphisms that vary along the East Coast of North America. We found a clear
249 signal of parallelism between seasonal and latitudinal variation in both the California and the Europe
250 comparisons: for the top 1% of seasonal and clinal polymorphism, 70% and 63% have parallel allele
251 frequency change, for California and Europe, respectively (greater than 100/100 and 99/100 matched
252 controls; Figure 2E).

253

254 As SNPs in or near a number of major inversions are enriched for seasonal variation (Figure 2D), we
255 tested whether there is increased seasonal and latitudinal parallelism in these regions. For the top 5%
256 of clinal and seasonal SNPs (n = 2132), parallel allele frequency change is highest near inversion
257 breakpoints on chromosomes 2L and 3R (92%, CI_{95}: 87-96%, and 86%, CI_{95}: 78-93%, respectively)
258 and inside the 2L inversion (83%, CI_{95}: 80-87%; Figure 2F). While parallelism is greatest overall
259 around inversion breakpoints (concordance: 81%, CI_{95}: 77-84%) and inside inversions (concordance:

260 70%, CI_{95}: 67-73%), we also observe a statistically significant excess of latitudinal and seasonal
261 parallelism outside of inversions (concordance: 57%, CI_{95}: 53-62%). The elevated signal of
262 parallelism between spatial and seasonal allele frequency fluctuations across the whole genome, and
263 in particular outside of inverted regions, suggests that inversions themselves, while important, are not
264 the sole drivers of allele frequency change between seasons.
265
266 **Predictability of seasonal adaptation based on local environmental conditions**
267 The signature of seasonal adaptation that we observe indicates that there are consistent changes in
268 allele frequencies between seasons, broadly defined, among populations sampled across multiple
269 years, and localities separated by thousands of miles (Figure 1A,B). Next, we asked if seasonal
270 fluctuations in allele frequencies are predictable within any particular population or year, and if the
271 extent of predictability is related to aspects of local climate or other factors.
272
273 To address this question, we performed a leave-one-out analysis. In this analysis, we sequentially
274 removed each of the 20 paired spring-fall populations within the Core20 set and re-identified
275 seasonally variable SNPs among the remaining 19 populations as well as for the dropped, 20th
276 population. To evaluate predictability, we calculated the proportion of SNPs that have the same
277 direction of allele frequency change between spring and fall in both the discovery and test models
278 (i.e., concordant allele frequency change). We estimated concordance across the range of joint
279 significance thresholds of both models. For each population, we then calculated a 'predictability
280 score'. This score reflects the change in concordance rate as a function of the joint significance
281 threshold (see Materials and Methods for details). Note that populations with a positive predictability
282 score are those in which the concordance rate is greater than 50% over the bulk of the genome or
283 chromosome.
284
285 We find that the majority of populations show a positive predictability score (Figure 3A). For these
286 populations, the concordance rate reaches 60-70% among SNPs passing a stringent joint significance
287 threshold (top 0.1% in both models). At more modest joint significance thresholds (e.g., the top 10%

in both sets), the concordance rate is lower but still statistically different from 50% (maximum nominal *p*-value at the top 5% of sites is 0.008). At the same time, intriguingly, we found that four of the 20 populations had negative predictability scores (Benton Harbor, Michigan 2014; Lancaster, Massachusetts 2012; Topeka, Kansas 2014; and Esparto, California 2012). Strong allele frequency changes in these four populations occur, but the direction of allele frequency change from spring to fall at many SNPs is opposite that of the remaining populations.

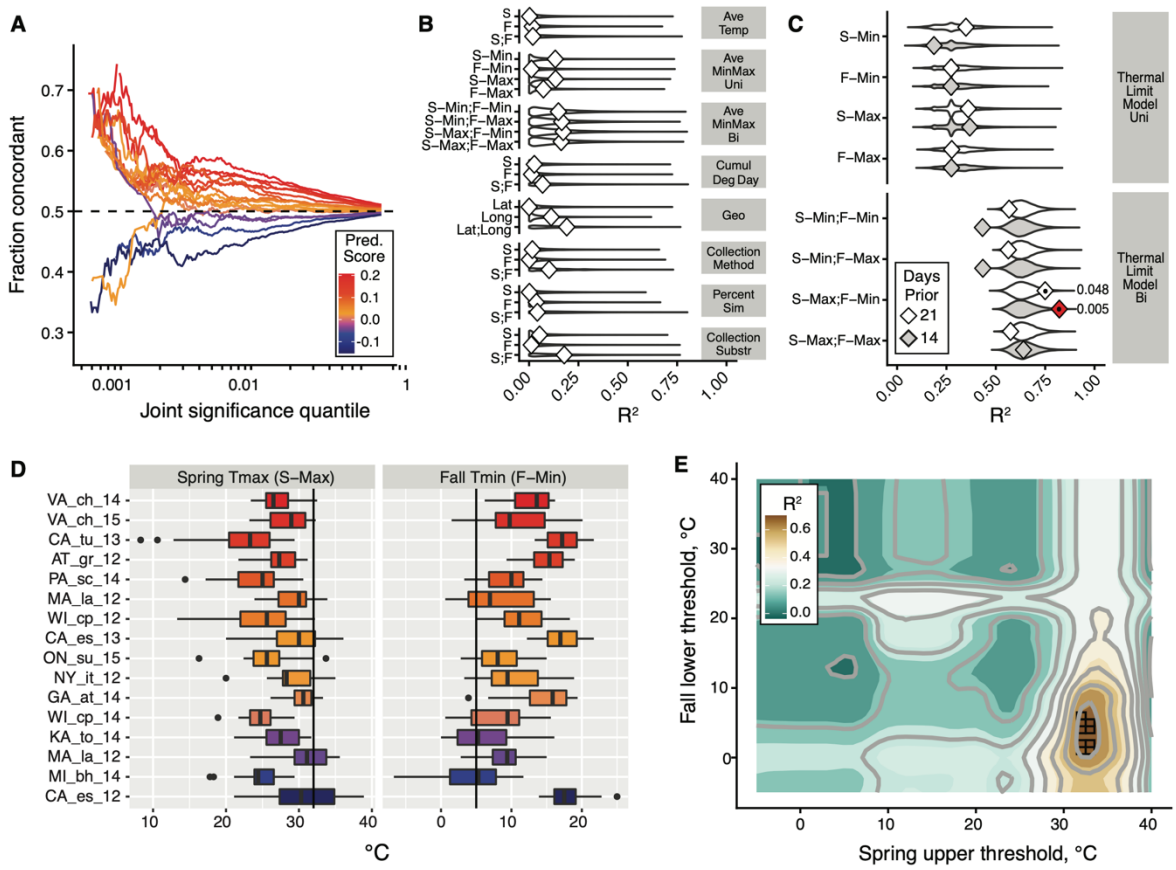

Figure 3. **The thermal limit model.** The thermal limit model argues that weather in the weeks prior to sampling can explain variation in the predictability of allele frequency change. (A) Each line represents the comparison between one population and the remaining 19. The x-axis represents the upper threshold of quantile-ranked *p*-values from the single-population test (Fisher's Exact Test) and the 19-population test (GLM), e.g. the top 1% in both tests. The y-axis is the fraction of SNPs where the sign of allele frequency change in the single population test matches the average sign change among the remaining 19. The color scheme represents the slope of this line and is used as a summary statistic for each population. (B/C). We regressed the summary score from (A) onto a number of characterizations of average temperature (B, first four rows), geography (B, 5th row), technical (B, rows 6-8), and thermal extremes (C), considering weather 14. Diamonds represent the observed R^2 for (B) and observed maximum R^2 across all thermal limits for (C). Violin plots represent the expected distribution of R^2 based on permutations. The red diamond represents the model with nominal *p*-value < 0.01. The empirical *p*-values for these models are listed next to the corresponding red diamond. The 14 day model that uses the counts of hot spring days and cold fall days passes a conservative application of the Bonferroni (see Results & Materials and Methods) at alpha = 0.13. (D) The

distribution of spring maximum (S- Max) daily temperature and fall minimum (F-min) daily temperature in the 2 weeks prior to sampling. Discordant (blue) populations do not cluster in time or space. Populations shown here are those in which we have weather data (15 populations, in total). (E) The stand-out model uses the number of hot spring days and cold fall days. To determine the optimal threshold for what defines hot and cold, we systematically varied the upper and lower thermal limits from 0°C to 40°C and used the count of hot spring (x1) and cold fall (x2) days as independent, additive variables in a regression model; the genome-wide predictability score was used as the dependent variable (y). The best fit model uses a spring max (S-Max) temp. of ~32°C and a fall min (F-Min) temp of ~5°C and explains ~82% of the variation in the population predictability scores.

We then asked why predictability scores vary among populations. To address this question we built models that related the genome-wide predictability score (Fig 3A) for each population with a number of different potential explanatory variables (Fig 3B,C,D). We first considered a number of nuisance variables such as collection method and substrate, as well as contamination rates by *D. simulans*. None of these variables are highly correlated with the genome-wide predictability score more than expected by chance (Fig 3B). Latitude and longitude are also not strong predictors of variation in genome-wide predictability score (Fig 3B).

We next focused on an environmental model based on aspects of the thermal environment. The motivation for these characterizations of temperature is based on the hypothesis that populations with negative genome-wide predictability scores were exposed to particularly warm springs and/or particularly cool falls prior to our sampling. This hypothesis is plausible considering that short-term changes in temperature have been linked, either directly or indirectly, to dramatic and partly predictable changes in allele frequencies in the wild and in the laboratory in multiple Drosophilid species (Barghi et al., 2019; Bergland et al., 2014; Mallard et al., 2018; Rodríguez-Trelles et al., 2013; Tobler et al., 2014). We evaluated a number of features of temperature by calculating daily averages, average minimum and maximums, as well as the cumulative degree days (Figure 3B). Finally, we calculated the number of days below and above thermal limits, with the thermal limits defined across a range of possible values (Fig 3C).

We find that the only set of features of the population that is significantly correlated with genome-wide predictability score is the number of hot spring days and number of cold fall days prior to

318 sampling. The best fit thermal limit model explains 82.2% of the variation in genome-wide
319 predictability scores (Figure 3C, 3E), beats >99.5% of permutations, and survives conservative
320 Bonferroni multiple-test correction at alpha=0.13 (Figure 3C). Specifically, the thermal limits
321 identified by this best fit model are the number of days in the two weeks prior to spring sampling with
322 maximum temperature above ~32°C and the number of days in the fall with minimum temperature
323 below ~5°C. These values roughly correspond to upper and lower thermal limits for flies (Hoffmann,
324 2010; Kellermann et al., 2012; Overgaard and MacMillan, 2017). Taken together, these results
325 suggest that exposure to temperature extremes, or to associated environmental variables, acts as a
326 selective pressure in the wild, causing large fluctuations in allele frequency throughout the genome.
327

328 ## ***Discussion***

329 In this study we have focused on the identification of genomic signatures of seasonal adaptation in *D.*
330 *melanogaster*. Our approach relies on the detection of parallel changes in allele frequency from spring
331 to fall across 20 populations. We use coarse definitions of spring and fall, with spring as the time of
332 year close to when *D. melanogaster* first becomes locally abundant and fall as the time close to the
333 end of the growing season but before populations become too scarce to sample (Behrman et al., 2015;
334 Ives, 1970). We sampled populations across a wide geographic range, such that the length of the
335 growing season as well as other environmental conditions varied substantially. Despite this
336 environmental heterogeneity and the coarseness of the definitions of spring and fall, we detect clear
337 signals of parallel seasonal allele frequency shifts across these populations (Figure 2A,B).
338 Specifically, we demonstrate that seasonal adaptation is a general phenomenon of temperate *D.*
339 *melanogaster* populations, and not restricted to a single orchard (Linvilla Orchard, Media,
340 Pennsylvania: Behrman et al., 2015; Bergland et al., 2014; Cogni et al., 2014; Schmidt and Conde,
341 2006), biogeographic region (East Coast of North America: Behrman et al., 2018), or even a
342 continent.
343

By detecting consistent seasonal changes in allele frequencies among multiple populations in North America and Europe we can argue that seasonal adaptation across this whole range is at least partly driven by a consistent set of loci. Note that at the moment we lack power to detect alleles that cycle in a small subset of populations or are private to a single population. We therefore focus only on the polymorphisms that segregate in all populations - and which consequently have a higher population frequency - and only look at the signal of parallel cycling. Thus, our conclusions are limited to the shared genetic basis of seasonal adaptation as revealed by the cycling of ~750,000 common SNPs which represent roughly half of all detected SNPs.

The detected seasonal SNPs can either be causal or, vastly more likely, linked to nearby causal genetic variants, be they SNPs, indels, structural variants, or transposable element insertions. While we cannot determine the precise number and identity of causal sites in the present study, the totality of the evidence is consistent with the polygenic nature of adaptation. Specifically, while we detected stronger seasonal signal near or inside several inversions on chromosomes 2L, 3L, and 3R suggesting that inversions are important drivers of seasonal adaptation (Dobzhansky, 1948, 1943; Kapun et al., 2016; Kapun and Flatt, 2019; Rodríguez-Trelles et al., 2013), we found that by focusing on the subset of seasonal sites that also show clinal patterns of geographic differentiation, we could detect seasonal signal outside inversions as well. Note that cosmopolitan inversions span a substantial portion of the genome and there is also likely to be substantial genetic diversity within these cytologically defined elements. Our study suggests that the strongly polygenic nature of seasonal adaptation will require a much broader seasonal sampling of populations to fine-map the causal variants and that such an endeavor is not futile, given that it is possible to detect a set of loci that show consistent seasonal fluctuations. At the same time, obtaining genomic data capable of identifying structural variation, including inversions, that plausibly underlie much of seasonal adaptation in *Drosophila* will clearly be important.

One key and poorly understood aspect of *Drosophila* seasonal adaptation is how the populations survive annual population collapse during the winter, manage to overwinter, and then manage to

372 expand and recolonize the available resources during the summer (Ives, 1970; Shpak et al., 2010).
373 Also poorly understood is the extent to which these patterns of collapse-overwintering-repopulation
374 involve migration and refugia (Coyne and Milstead, 1987; Ives, 1970). However, it is clear that
375 seasonal adaptation in *D. melanogaster* cannot involve wholesale population replacements by
376 migration because the spatial structure of the *D. melanogaster* populations is robust year after year as
377 evidenced by strong spatial population structure (Figure 1C) and persistent clinal patterns (Machado
378 et al., 2016; van Heerwaarden and Hoffmann, 2007). While one can conceive of migration from local
379 refugia playing a role, any such scenario still requires natural selection to operate in order to reset
380 populations back to the "spring" state every year. The full metapopulation dynamics and the ways that
381 local *D. melanogaster* survive seasonal crashes and expansions remains to be understood.
382
383 Our ability to detect a shared genetic basis of seasonal adaptation across these broadly distributed
384 populations implies that there are generic features in the environment that exert consistent selective
385 pressures despite the environmental heterogeneity across sampling times and locations. It is possible
386 that such generic selective pressures relate to temperature, humidity, population density, resource
387 availability, or other biotic and abiotic factors (Bogaerts-Márquez et al., 2020). The seasonal and
388 latitudinal parallelism in allele frequency change that we observe (Figure 2E) suggests that the
389 environmental factors that drive these patterns must both shift between seasons locally and vary
390 spatially from south to north.
391
392 While the exact nature of the environmental variables that drive seasonal selection remain to be
393 determined, here we provide evidence that temperature extremes in the weeks prior to sampling are a
394 strong proximate or even ultimate selective agent (Figure 3). Specifically, we show that the seasonal
395 behavior of any one population could be statistically associated with temperature extremes in the 2
396 weeks prior to sampling both in the spring and in the fall. This model accounts for why several
397 populations showed reversal of direction of movement of seasonal SNPs relative to the bulk of the
398 populations; these populations had unusually warm springs and unusually cool falls prior to sampling.
399 We thus hypothesize that, at the time of sampling, some of our spring samples had already

experienced sufficiently strong selection in the generically summer way and that the fall samples had experienced selective pressures in the generically winter way. This would result in seasonal alleles in the spring already showing fall-like patterns and the ones in the fall showing spring-like patterns.

These findings also raise an intriguing possibility that natural selection may not push populations in the same consistent direction across the entire growing season but rather that natural selection and adaptation may be more heterogeneous through time (Grant and Grant, 2002; Nosil et al., 2020; Siepielski et al., 2009). In the future, more dense temporal sampling might help map the action of natural selection to more specific environmental factors and to quantify how fast the selective pressures change in strength and even direction across a single growing season. Our results thus illustrate that evolution and ecology do operate on similar timescales in this system (Hendry, 2020; Schoener, 2011; Thompson, 1998; Yoshida et al., 2003) and that evolutionary adaptation cannot be generally ignored *a priori* in demographic or ecological investigations even on extremely short timescales (Rudman et al., 2018)

While the number of detected seasonal loci is likely to be a vast overestimate of the number of causal seasonal variants, the strength of selection implied by the magnitude of fluctuations at seasonal sites while already high is likely to be an underestimate. Partially linked loci should show a smaller magnitude of fluctuation than the true causal sites. Thus the 4-8% seasonal frequency shifts at the top 1% of the seasonal sites and the corresponding effective selection coefficients of ~10-30% per season (~1-3% per generation) imply even larger magnitudes of selection at the causal sites. Furthermore, given that we can only detect patterns of seasonal cycling that are at least partially consistent across all or most sampled populations we are likely to underestimate the impact of linked seasonal selection due to selection that is occurring in a population-specific manner. Seasonal adaptation therefore likely constitutes a profound evolutionary force acting on a large number of dispersed loci and affecting linked variation genome-wide. This seasonal selection force could rival in strength genetic draft due to selective sweeps and should be much stronger over seasonal timescales than random genetic drift in populations as large as *D. melanogaster* (Karasov et al., 2010).

428

429 Our observation that seasonal adaptation is polygenic and rapid suggests that there exists a substantial
430 number of common polymorphisms that are subject to strong fluctuating selection that are nonetheless
431 maintained across the range of *D. melanogaster*. The most straightforward explanation of these results
432 is that these polymorphisms are subject to some form of balancing selection (Bertram and Masel,
433 2019; Charlesworth, 2015; Gulisija and Kim, 2015, Levene, 1953; Wittmann et al., 2017). Pervasive
434 balancing selection is consistent with the recent realization that simple models of mutation-selection
435 balance are inconsistent with the extent of quantitative genetic variation in a variety of fitness related
436 traits (Charlesworth, 2015). A full understanding of the genomic consequences of balancing selection
437 caused by strong fluctuating selection will require the identification of individual causal loci. Doing
438 so will require substantial additional sampling across seasons as well as from closely and broadly
439 distributed locales throughout the whole geographic range of *D. melanogaster* in combination with
440 the genetic mapping of seasonally fluctuating phenotypes (Behrman et al., 2018, 2015; Erickson et al.,
441 2020; Rajpurohit et al., 2018, 2017; Schmidt and Conde, 2006). Finally, such efforts can be strongly
442 augmented by manipulative field experiments and functional work to investigate the molecular effects
443 of putatively causal genetic variants. All of this work will need to be done in the context of other
444 processes that underlie persistence of populations in the face of environmental heterogeneity such as
445 phenotypic plasticity and bet hedging (Ayrinhac et al., 2004; Bergland et al., 2008; Kain et al., 2015;
446 MacMillan et al., 2015; Overgaard et al., 2011; Via and Lande, 1985). Overall, it is becoming clear
447 that all of the key ecological and evolutionary processes, including demographic changes, mutation,
448 migration, phenotypic plasticity, and rapid evolution by natural selection, can and do occur on very
449 short and overlapping timescales and thus must be investigated as part of one complex evolving and
450 interacting system.

451

452 ## ***Materials and methods***

453 **Population sampling and sequence data**

454 We assembled 73 samples of *D. melanogaster*, 61 representing newly collected and sequenced
455 samples and 12 representing previously published samples (Bergland et al., 2014; Kapun et al., 2016).
456 Locations, collection dates, number of individuals sampled, and depth of sequencing for all samples
457 are listed in Supplemental Table 1. For each sample, members of the Drosophila Real-Time Evolution
458 Consortium (DrosRTEC) collected an average of 75 male flies using direct aspiration from substrate,
459 netting, or trapping at orchards and residential areas. Flies were confirmed to be *D. melanogaster* by
460 examination of the male genital arch. We extracted DNA by first pooling all individuals from a
461 sample, grinding the tissue together in extraction buffer, and using a lithium chloride – potassium
462 acetate extraction protocol (see Bergland et al. 2014 for details on buffers and solutions). We prepared
463 sequencing libraries using a modified Illumina protocol (Bergland et al., 2014) and Illumina TrueSeq
464 adapters. Paired-end 125bp libraries were sequenced to an average of 94x coverage either at the
465 Stanford Sequencing Service Center on an Illumina HiSeq 2000, or at the Stanford Functional
466 Genomics facility on an Illumina HiSeq 4000.
467
468 The following sequence data processing was performed on both the new and the previously published
469 data. We trimmed low-quality 3' and 5' read ends (sequence quality < 20) using the program cutadapt
470 v1.8.1 (Martin, 2011). We mapped the raw reads to the *D. melanogaster* genome v5.5 (and for *D.*
471 *simulans* genome v2.01, flybase.org) using bwa v0.7.12 mem algorithms, with default parameters (Li
472 & Durbin, 2009), and used the program SAMtools v1.2 for bam file manipulation (functions index,
473 sort, and mpileup) (Li et al., 2009). We used the program picard v2.0.1 to remove PCR duplicates
474 (http://picard.sourceforge.net) and the program GATK v3.2-2 for indel realignment (McKenna et al.,
475 2010). We called SNPs and indels using the program VarScan v2.3.8 using a *p*-value of 0.05,
476 minimum variant frequency of 0.005, minimum average quality of 20, and minimum coverage of 10
477 (Koboldt et al., 2012). We filtered out SNPs within 10bp of an indel (they are more likely to be
478 spurious), variants in repetitive regions (identified by RepeatMasker and downloaded from the UCSC
479 Genome browser), SNPs with a median frequency of less than 1% across populations, regions with
480 low recombination rates (~0 cM/Mb; Comeron et al., 2012), and nucleotides with more than two
481 alleles. Because we sequenced only male individuals, the X chromosome had lower coverage and was

482 not used in our analysis. After filtering, we had a total of 1,763,522 autosomal SNPs. This set was
483 further filtered to include only SNPs found polymorphic in all samples ("common polymorphisms"),
484 resulting in 774,651 SNPs that represent the core set used in our analyses.
485
486 Due to the phenotypic similarity of the species *D. melanogaster* and *D. simulans*, we tested for *D.*
487 *simulans* contamination by competitively mapping reads to both genomes. We omitted any of our
488 pooled samples with greater than 5% of reads mapping preferentially to *D. simulans* (Charlottesville,
489 VA 2012, fall; Media, PA 2013 fall). For the remaining samples, reads that mapped better to the *D.*
490 *simulans* were removed from the analysis. For the populations used in this analysis, the average
491 proportion of reads mapping preferentially to *D. simulans* was less than 1% (see Supplemental Table
492 1), and there was no significant difference in the level of *D. simulans* contamination between spring
493 and fall samples (*t*-test $p = 0.90$).
494
495 In silico simulation analysis shows that competitive mapping accurately estimates the fraction of *D.*
496 *simulans* contamination. To conduct these simulations, we used a single *D. simulans* genome from an
497 inbred line derived from an individual caught California (Signor et al., 2017) and a single *D.*
498 *melanogaster* genome from a DGRP line (Mackay et al., 2012). We used wgsim to generate simulated
499 short-reads from each genome and mixed these short reads together in various proportions. We then
500 mapped the short reads back to the composite genome for competitive mapping, as described above.
501 We calculated contamination rate as the number of total reads mapping to the *D. simulans* reference
502 genome divided by the number of reads mapping to both *D. simulans* and *D. melanogaster*. We also
503 calculated the locus specific residual cross mapping rate by calculating the number of *D. simulans*
504 reads that still map to the *D. melanogaster* genome even after competitive mapping. These
505 simulations demonstrate that the estimation of the cross species mapping is precise (Pearson's $r =$
506 0.9999, $p = 1.6 \times 10^{-24}$, Supplemental Figure 7A), but underestimates the true contamination rate by
507 ~2%. The level of residual *D. simulans* contamination does not correlate with contamination rate and
508 is roughly 9% (Supplemental Figure 7B).
509

510 To assess seasonal variation we analyzed population genomic sequence data from 20 spring and 20
511 fall samples ('Core20'). These samples represent a subset of the sequenced samples. We used samples
512 that had both a spring and a fall collection taken from the same locality in the same year. We also
513 used a maximum of two years of samples for a given locality to prevent the analysis from being
514 dominated by characteristics of a single population. When there were more than two years of samples
515 for a given population, we chose to use the two years with the earliest spring collection time. This
516 decision was made on the assumption that the earlier spring collection would better represent allele
517 frequencies following overwintering selection. This left 20 paired spring/fall samples, taken from 12
518 North American localities spread across 6 years and 3 European localities across 2 years
519 (Supplemental Table 1). The localities and years of sampling are as follows: Esparto, California 2012
520 and 2013; Tuolumne, California 2013; Lancaster, Massachusetts 2012 and 2014; Media, Pennsylvania
521 2010 and 2011; Ithaca, New York 2012; Cross Plains, Wisconsin 2012 and 2014; Athens, Georgia
522 2014; Charlottesville, Virginia 2014 and 2015, State College, Pennsylvania 2014; Topeka, Kansas
523 2014; Sudbury, Ontario, Canada 2015; Benton Harbor, Michigan 2014, Barcelona, Spain 2012;
524 Gross-Enzersdorf, Vienna 2012; Odesa, Ukraine 2013. For comparison of seasonal with latitudinal
525 variation, we used sequence data from four spring samples along the east coast of the United States
526 (Homestead, Florida 2010; Hahia, Georgia 2008; Eutawville, South Carolina 2010, Linvilla,
527 Pennsylvania 2009). We performed a principal components analysis of allele frequency per SNP per
528 sample using the prcomp function in R.
529
530 **Identification of seasonal sites**
531 We identified seasonal sites using three separate methods: a general linear regression model (GLM), a
532 Bayesian model (Bayenv; Coop et al., 2010; Günther & Coop, 2013) and a model based on the rank
533 Fisher's method (RFM). Statistical analyses were performed in R (R Core Team, 2014).
534
535 To perform the GLM we used the glm function with binomial error, weighted by the "effective
536 coverage" (N_c)- a measure of the number of chromosomes sampled, adjusted by the read depth:
537 $$N_c = (1/N + 1/R)-1$$

538 where N is the number of chromosomes in the pool and R is the read depth at that site (Kolaczkowski
539 et al., 2011; Feder et al., 2012; Bergland et al., 2014; Machado et al., 2016). This adjusts for the
540 additional error introduced by sampling of the pool at the time of sequencing. The seasonal GLM is a
541 regression of allele frequency by season (e.g., spring versus fall):

542 $$y_i = \text{season} + \text{population} + e_i$$

543 where y_i is the allele frequency at the ith SNP, population is the unordered categorical variable
544 denoting each of the 20 populations, and ei is the binomial error at the ith SNP. Although the GLM is
545 a powerful test, the corrected binomial sampling variance (N_c) is likely an anti-conservative estimate
546 of the true sampling variance associated with pooled sequencing (Machado et al., 2016; Spitzer et al.,
547 2019). Therefore, we use the results of this test as a seasonal outlier test, rather than an absolute
548 measure of the deviation from genome-wide null expectation of no allele frequency change between
549 seasons. Results are compared to 500 permutations of the spring and fall labels within each population
550 pair.
551
552 We tested for signals of seasonality using Bayenv. First, we calculated the genetic-covariance matrix
553 between the Core20 set. Next, we calculated Bayes Factor scores for each SNP using the observed
554 spring and fall labels. We used the read counts of reference and alternate based on the corrected
555 binomial sampling variance (N_c). We conducted 100 permutations of the spring and fall labels within
556 each population pair.
557
558 Finally, we developed a test to identify signals of seasonality which we call the "Rank Fisher's
559 Method" (RFM) that is robust to the inflated sample size estimates that can arise when using pooled
560 allele frequencies (Machado et al., 2016). For this method, we first perform a Fisher's Exact Test for
561 spring-fall allele frequency differentiation within each population pair. We then rank-normalize the
562 resulting *p*-values for any given population by grouping SNPs into categories based on the number of
563 total number of reads and the number of alternate reads, summed between spring and fall. The class-
564 based rank of each SNP becomes its new *p*-value, providing uniform sets of *p*-values across the
565 genome. As the power (minimum *p*-value) is relative to the number of SNPs being ranked per bin,

566 and as the bin sizes are equivalent across populations, each population has equivalent power.
567 Additionally, we find that this method is robust to inaccurate estimates of allele frequency precision
568 (Supplemental Figure 8). We then combine ranked *p*-values using Fisher's method for each SNP,
569 taking two times the negative sum of logged *p*-values across the 20 spring/fall comparisons (each tail
570 tested separately). The null distribution for this statistic (X^2) is a Chi-squared distribution with
571 degrees of freedom equal to 40 (two times the number of comparisons). We used the distribution of
572 these per-SNP X^2 test statistics to test for a seasonal signal above noise and compared to 200
573 spring/fall permutations.
574
575 **Inversions**
576 We analyzed seasonal variation associated with 6 major cosmopolitan inversions found in *D.*
577 *melanogaster*: *In(2L)t* (2L:2225744-13154180), *In(2R)NS* (2R:11278659-16163839), *In(3L)P*
578 (3L:3173046-16301941), *In(3R)K* (3R:7576289-21966092), *In(3R)Mo* (3R:17232639-24857019),
579 *In(3R)P* (3R:12257931-20569732). As the three inversions on 3R are overlapping, we combined
580 them. We classified the genome into three categories- inversion breakpoints (500Kb +/- each
581 inversion breakpoint; 104K SNPs), inside inversions (excluding breakpoint regions; 390K SNPs) and
582 outside inversions (excluding breakpoint regions; 281K SNPs).
583
584 **Matched controls**
585 With the assumption that the majority of the genome is not seasonal, we can use matched genomic
586 controls as a null distribution to test for enrichment of different features of seasonal polymorphisms.
587 The use of matched control SNP sets was employed for the tests of seasonal and latitudinal
588 parallelism. We matched each SNP identified as significantly seasonal (at a range *p*-values) to another
589 SNP, matched for chromosome, effective coverage, median spring allele frequency, inversion status
590 either within or outside of the major inversions *In(2L)t*, *In(2R)NS*, *In(3L)P*, *In(3R)K*, *In(3R)Mo*, and
591 *In(3R)P*, and recombination rate. We used the same *D. melanogaster* inversion breakpoints used in
592 Corbett-Detig & Hartl (2012) and the recombination rates from Comeron et al. (2012). We randomly
593 sampled 100 of the possible matches per SNP (excluding the focal SNP) to produce 100 matched

594 control sets. Any SNPs with fewer than 10 possible matches were discarded from the matched control
595 analyses. We defined 95% confidence intervals from the matched controls as the 3rd and 98th ranked
596 values for the quantity being tested (e.g., percent concordance or proportion of genic classes).
597
598 **Latitudinal cline concordance**
599 To identify SNPs that changed consistently in allele frequency with latitude (clinal), we first
600 identified SNPs that varied in allele frequency along a 14.4° latitudinal transect up the east coast of
601 the United States. We used one spring sample from each of the following populations (identified as
602 "Region_City_Year"): PA_li_2011 (39.9°N), SC_eu_2010 (33.4°N), GA_ha_2008 (30.1°N), and
603 FL_ho_2010 (25.5°N).
604
605 First, we regressed allele frequency with population latitude in a general linear model (glm: R v3.1.0),
606 using a binomial error model and weights proportional to the effective coverage (N_c):
607 $$y_i = \text{latitude} + e_i$$
608 where y_i is the allele frequency at the ith SNP, and e_i is the binomial error given the ith at the SNP. To
609 confirm the robustness of the clinal GLM results, clinality also was assessed using a second, more
610 complex model that accounts for existing covariance in the dataset (Bayenv: Coop et al., 2010;
611 Günther & Coop, 2013).
612
613 We then tested the concordance in allele frequency change by season with the allele frequency change
614 by latitude. We performed three separate seasonal regressions (see above) for comparison with the
615 latitudinal regression: spring verses fall for the 18 non-Pennsylvania paired samples, spring versus fall
616 for the three California paired samples, and spring versus fall for the three Europe paired samples.
617 With the removal of the Pennsylvania samples, none of these three seasonal regressions contained
618 samples from any of the four populations used for the latitudinal regression. Taking sets of
619 increasingly clinal and increasingly seasonal SNPs, we assessed the proportion of sites that both
620 increase in frequency from spring to fall and increase in frequency from north to south or that

621 decrease in frequency from spring to fall and decrease in frequency from north to south. We
622 compared this concordance with the concordance of 100 sets of matched controls.
623
624 **Predictability analysis**
625 To test the general predictability of seasonal change in our dataset, we performed a leave-one-out
626 analysis. In this analysis, we performed seasonal regressions for subsets of the data, dropping one
627 paired sample and comparing it to a seasonal test of the remaining 19. For the single population
628 model, we used a Fisher's exact test. For the multi-population model, we used a generalized linear
629 model. For either model, we used the effective number of reads (N_c, defined above). We then
630 measured the percent concordance of spring/fall allele frequency change, defined as the proportion of
631 SNPs that agree in the direction of allele frequency change between spring and fall. This was
632 performed 20 times, once for each paired sample.
633
634 To estimate the predictability scores, we calculated the rate of change of the concordance score as a
635 function of quantile threshold. To estimate this rate, we used the generalized linear model with
636 binomial error,
637 $$\text{concordance}_i = \text{quantile}_i + e_i,$$
638 where 'concordance' is the fraction of SNPs falling below the ith quantile threshold of both the target
639 (19 population) and test (1 population) models that changed in frequency in a concordant fashion and
640 e is the binomial error with weights corresponding to the total number of SNPs falling below that
641 threshold. Thus, the genome-wide (or chromosome specific) predictability score is heavily influenced
642 by concordance rates of higher quantiles because that is where the bulk of SNPs reside.
643
644 We tested whether the variation in genome-wide predictability scores among populations is correlated
645 with different features of the samples. We evaluated different nuisance parameters, such as collection
646 method, substrate, and *D. simulans* contamination rate, as well as a number of features related to
647 temperature. Daily minimum and maximum temperatures were obtained from the Global Historical
648 Climatology Network-Daily Database (Menne et al., 2012). We matched each locality to a weather

649 station based on geographic distance. For the Core20 set of populations, four of the collections did not
650 have precise collection dates for one or both seasonal collections (Athens, Georgia 2014; Media,
651 Pennsylvania 2010, 2011; Barcelona, Spain 2012), or were not associated with any climate data from
652 the GHCND database (Odessa, Ukraine 2013). These five populations were omitted from the analysis,
653 leaving 15 populations for the remainder of the predictability analysis (Figure 3D). Using daily
654 temperature data, we calculated the cumulative growing degree days following a model developed for
655 *D. suzukii* by Wiman et al (2014).
656
657 We regressed the predictability score onto each potential explanatory variable, recorded the
658 proportion of variation explained (R^2), and contrasted the observed R^2 to null distributions generated
659 via permutation (n = 25,000). For most variables, we performed a univariate model (e.g., latitude or
660 longitude). In some cases, we used a bivariate model (e.g., latitude + longitude). To test the thermal
661 limit model, we regressed the observed predictability score on the number of days above and below
662 the thermal limits. We varied thermal limits from -5°C to 40°C with a step size of 0.1°C.
663
664 **Data availability**
665 All raw sequence data have been deposited to the NCBI short read archive (SRA; BioProject
666 Accession #PRJNA308584; accession numbers for each sample can be found in Supplemental Table
667 1). Code to conduct these analyses, primary results files, and code to reproduce the figures are
668 available at https://github.com/machadoheather/dmel_seasonal_RTEC. VCF files with the raw allele
669 frequencies per population and a R-data file of allele frequencies and effective sample sizes (N_c;
670 compatible with scripts) are available on DataDryad
671 (https://datadryad.org/stash/dataset/doi:10.5061/dryad.4r7b826).
672

673 ## ***Acknowledgements***

674 We thank the National Evolutionary Synthesis Center (NESCent) for sponsoring the 2012 Catalysis
675 meeting that initiated the *Drosophila* Real Time Evolution Consortium. The meeting was attended by

Alan Bergland, Alisa Sedghifar, Brian Helmuth, Brian Lazzarro, Chau-Ti Ting, David Kidd, Dmitri Petrov, Fabian Staubach, Hannah Burrack, Jim Fry, John Lessard, John Coulbourne, John Pool, Josefa Gonzalez, Julien Ayroles, Kelly Dyer, Kim Hughes, Maaria Kankare, Nadia Singh, Paul Schmidt, Regan Early, Stephen Porder, Subhash Rajpurohit, Sui Fai Lee, and Thomas Flatt, and we kindly thank all participants for their participation. We also thank Jamie Blundell and all members of the Schmidt and Petrov labs who provided exceptionally valuable feedback. This work was funded by the NIH grants R01GM100366 to PS and DAP, R35GM118165 to DAP, R01GM100366 to PS, F32GM097837 and R35GM119686 to AOB, European Commission grant H2020-ERC-2014-CoG-647900 to JG, a NSERC Discovery Grant RGPIN-2018-05551 and Canada Research Chair 950-230113 to TJSM.

Author contributions

Heather E. Machado: Designed the study, collected flies, performed analysis, wrote manuscript; Alan O. Bergland: Designed the study, collected flies, performed analysis, wrote manuscript; Ryan Taylor: Performed analysis; Susanne Tilk: Prepared sequencing libraries; Emily Behrman: Collected flies; Kelly Dyer: Collected flies; Daniel K. Fabian: Collected flies; Thomas Flatt: Collected flies; Josefa González: Collected flies; Talia L. Karasov: Collected flies; Iryna Kozeretska: Collected flies; Brian P. Lazzaro: Collected flies; Thomas JS Merritt: Collected flies; John E. Pool: Collected flies; Katherine O'Brien: Collected flies; Subhash Rajpurohit: Collected flies; Paula R. Roy: Collected flies; Stephen W. Schaeffer: Collected flies; Svitlana Serga: Collected flies; Paul Schmidt: Designed the study, collected flies, wrote manuscript; Dmitri Petrov: Designed the study, collected flies, wrote manuscript. All authors edited and approved the manuscript.

References

Ayrinhac A, Debat V, Gibert P, Kister A-G, Legout H, Moreteau B, Vergilino R, David JR. 2004. Cold adaptation in geographical populations of *Drosophila melanogaster*: phenotypic plasticity is more important than genetic variability. *Funct Ecol* **18**:700–706. doi:10.1111/j.0269-8463.2004.00904.x

Barghi N, Tobler R, Nolte V, Jakšić AM, Mallard F, Otte KA, Dolezal M, Taus T, Kofler R, Schlötterer C. 2019. Genetic redundancy fuels polygenic adaptation in *Drosophila*. *PLoS Biol*

17:e3000128. doi:10.1371/journal.pbio.3000128
Behrman EL, Howick VM, Kapun M, Staubach F, Bergland AO, Petrov DA, Lazzaro BP, Schmidt PS. 2018. Rapid seasonal evolution in innate immunity of wild *Drosophila melanogaster*. *Proc Biol Sci* **285**. doi:10.1098/rspb.2017.2599
Behrman EL, Watson SS, O'Brien KR, Heschel MS, Schmidt PS. 2015. Seasonal variation in life history traits in two *Drosophila* species. *J Evol Biol* **28**:1691–1704. doi:10.1111/jeb.12690
Bergland AO, Behrman EL, O'Brien KR, Schmidt PS, Petrov DA. 2014. Genomic evidence of rapid and stable adaptive oscillations over seasonal time scales in *Drosophila*. *PLoS Genet* **10**:e1004775. doi:10.1371/journal.pgen.1004775
Bergland AO, Genissel A, Nuzhdin SV, Tatar M. 2008. Quantitative trait loci affecting phenotypic plasticity and the allometric relationship of ovariole number and thorax length in *Drosophila melanogaster*. *Genetics* **180**:567–582. doi:10.1534/genetics.108.088906
Bertram J, Masel J. 2019. Different mechanisms drive the maintenance of polymorphism at loci subject to strong versus weak fluctuating selection. *Evolution* **73**:883–896. doi:10.1111/evo.13719
Bogaerts-Márquez M, Guirao-Rico S, Gautier M, González J. 2020. Temperature, rainfall and wind variables underlie environmental adaptation in natural populations of *Drosophila melanogaster*. *Mol Ecol*. doi:10.1111/mec.15783
Botero CA, Weissing FJ, Wright J, Rubenstein DR. 2015. Evolutionary tipping points in the capacity to adapt to environmental change. *Proc Natl Acad Sci* **112**:184–189. doi:10.1073/pnas.1408589111
Buffalo V, Coop G. 2020. Estimating the genome-wide contribution of selection to temporal allele frequency change. *Proc Natl Acad Sci U S A* **117**:20672–20680. doi:10.1073/pnas.1919039117
Bürger R, Gimelfarb A. 1999. Genetic variation maintained in multilocus models of additive quantitative traits under stabilizing selection. *Genetics* **152**:807–820.
Campo D, Lehmann K, Fjeldsted C, Souaiaia T, Kao J, Nuzhdin SV. 2013. Whole-genome sequencing of two North American *Drosophila melanogaster* populations reveals genetic differentiation and positive selection. *Mol Ecol* **22**:5084–5097. doi:10.1111/mec.12468
Charlesworth B. 2015. Causes of natural variation in fitness: evidence from studies of *Drosophila* populations. *Proc Natl Acad Sci U S A* **112**:1662–1669. doi:10.1073/pnas.1423275112
Cogni R, Kuczynski C, Koury S, Lavington E, Behrman EL, O'Brien KR, Schmidt PS, Eanes WF. 2014. The intensity of selection acting on the couch potato gene--spatial-temporal variation in a diapause cline. *Evol Int J Org Evol* **68**:538–548. doi:10.1111/evo.12291
Cogni R, Kuczynski K, Lavington E, Koury S, Behrman EL, O'Brien KR, Schmidt PS, Eanes WF. 2015. Variation in *Drosophila melanogaster* central metabolic genes appears driven by natural selection both within and between populations. *Proc Biol Sci* **282**:20142688. doi:10.1098/rspb.2014.2688
Comeron JM, Ratnappan R, Bailin S. 2012. The Many Landscapes of Recombination in *Drosophila melanogaster*. *PLOS Genet* **8**:e1002905. doi:10.1371/journal.pgen.1002905
Coop G, Witonsky D, Rienzo AD, Pritchard JK. 2010. Using Environmental Correlations to Identify Loci Underlying Local Adaptation. *Genetics* **185**:1411–1423. doi:10.1534/genetics.110.114819
Corbett-Detig RB, Hartl DL. 2012. Population Genomics of Inversion Polymorphisms in *Drosophila melanogaster*. *PLOS Genet* **8**:e1003056. doi:10.1371/journal.pgen.1003056
Coyne JA, Milstead B. 1987. Long-Distance Migration of *Drosophila*. 3. Dispersal of *D. melanogaster* Alleles from a Maryland Orchard. *Am Nat* **130**:70–82. doi:10.1086/284698
Curtsinger JW, Service PM, Prout T. 1994. Antagonistic Pleiotropy, Reversal of Dominance, and Genetic Polymorphism. *Am Nat* **144**:210–228. doi:10.1086/285671
Denlinger DL. 2002. Regulation of Diapause. *Annu Rev Entomol* **47**:93–122. doi:10.1146/annurev.ento.47.091201.145137
Dobzhansky T. 1948. Genetics of natural populations; altitudinal and seasonal changes produced by natural selection in certain populations of *Drosophila persimilis*. *Genetics* **33**:158–176.
Dobzhansky T. 1943. Genetics of Natural Populations IX. Temporal Changes in the Composition of Populations of *Drosophila pseudoobscura*. *Genetics* **28**:162–186.

762 Ellner S. 1996. Environmental fluctuations and the maintenance of genetic diversity in age or stage-
763 structured populations. *Bull Math Biol* **58**:103–127. doi:10.1007/BF02458284
764 Ellner S, Hairston, NG. 1994. Role of Overlapping Generations in Maintaining Genetic Variation in a
765 Fluctuating Environment. *Am Nat* **143**:403–417. doi:10.1086/285610
766 Ellner S, Sasaki A. 1996. Patterns of Genetic Polymorphism Maintained by Fluctuating Selection with
767 Overlapping Generations. *Theor Popul Biol* **50**:31–65. doi:10.1006/tpbi.1996.0022
768 Erickson PA, Weller CA, Song DY, Bangerter AS, Schmidt P, Bergland AO. 2020. Unique genetic
769 signatures of local adaptation over space and time for diapause, an ecologically relevant
770 complex trait, in *Drosophila melanogaster*. *PLoS Genet* **16**:e1009110.
771 doi:10.1371/journal.pgen.1009110
772 Ewing EP. 1979. Genetic Variation in a Heterogeneous Environment VII. Temporal and Spatial
773 Heterogeneity in Infinite Populations. *Am Nat* **114**:197–212. doi:10.1086/283468
774 Fabian DK, Kapun M, Nolte V, Kofler R, Schmidt PS, Schlötterer C, Flatt T. 2012. Genome-wide
775 patterns of latitudinal differentiation among populations of *Drosophila melanogaster* from
776 North America. *Mol Ecol* **21**:4748–4769. doi:https://doi.org/10.1111/j.1365-
777 294X.2012.05731.x
778 Feder AF, Petrov DA, Bergland AO. 2012. LDx: Estimation of Linkage Disequilibrium from High-
779 Throughput Pooled Resequencing Data. *PLoS ONE* **7**:e48588.
780 doi:10.1371/journal.pone.0048588
781 Grant PR, Grant BR. 2002. Unpredictable evolution in a 30-year study of Darwin's finches. *Science*
782 **296**:707–711. doi:10.1126/science.1070315
783 Grenier JK, Arguello JR, Moreira MC, Gottipati S, Mohammed J, Hackett SR, Boughton R,
784 Greenberg AJ, Clark AG. 2015. Global diversity lines - a five-continent reference panel of
785 sequenced *Drosophila melanogaster* strains. *G3 Bethesda Md* **5**:593–603.
786 doi:10.1534/g3.114.015883
787 Günther T, Coop G. 2013a. Robust identification of local adaptation from allele frequencies. *Genetics*
788 **195**:205–220. doi:10.1534/genetics.113.152462
789 Günther T, Coop G. 2013b. Robust Identification of Local Adaptation from Allele Frequencies.
790 *Genetics* **195**:205–220. doi:10.1534/genetics.113.152462
791 Hager ER, Harringmeyer OS, Wooldridge TB, Theingi S, Gable JT, McFadden S, Neugeboren B,
792 Turner KM, Hoekstra HE. 2021. A chromosomal inversion drives evolution of multiple
793 adaptive traits in deer mice. *bioRxiv* 2021.01.21.427490. doi:10.1101/2021.01.21.427490
794 Hedrick PW. 1976. Genetic variation in a heterogeneous environment. II. Temporal heterogeneity and
795 directional selection. *Genetics* **84**:145–157.
796 Hendry AP. 2020. Eco-Evolutionary Dynamics. Princeton; Jackson: Princeton University Press Two
797 Rivers Distribution.
798 Hoffmann AA. 2010. Physiological climatic limits in *Drosophila*: patterns and implications. *J Exp*
799 *Biol* **213**:870–880. doi:10.1242/jeb.037630
800 Ives PT. 1970. Further genetic studies of the South Amherst population of *Drosophila melanogaster*.
801 *Evol Int J Org Evol* **24**:507–518. doi:10.1111/j.1558-5646.1970.tb01785.x
802 Jones FC, Grabherr MG, Chan YF, Russell P, Mauceli E, Johnson J, Swofford R, Pirun M, Zody MC,
803 White S, Birney E, Searle S, Schmutz J, Grimwood J, Dickson MC, Myers RM, Miller CT,
804 Summers BR, Knecht AK, Brady SD, Zhang H, Pollen AA, Howes T, Amemiya C, Lander
805 ES, Palma FD, Lindblad-Toh K, Kingsley DM. 2012. The genomic basis of adaptive
806 evolution in threespine sticklebacks. *Nature* **484**:55–61. doi:10.1038/nature10944
807 Kain JS, Zhang S, Akhund-Zade J, Samuel ADT, Klein M, Bivort BL. 2015. Variability in thermal
808 and phototactic preferences in *Drosophila* may reflect an adaptive bet-hedging strategy.
809 *Evolution* **69**:3171–3185. doi:10.1111/evo.12813
810 Kao JY, Zubair A, Salomon MP, Nuzhdin SV, Campo D. 2015. Population genomic analysis
811 uncovers African and European admixture in *Drosophila melanogaster* populations from the
812 south-eastern United States and Caribbean Islands. *Mol Ecol* **24**:1499–1509.
813 doi:10.1111/mec.13137
814 Kapun M, Barrón MG, Staubach F, Obbard DJ, Wiberg RAW, Vieira J, Goubert C, Rota-Stabelli O,
815 Kankare M, Bogaerts-Márquez M, Haudry A, Waidele L, Kozeretska I, Pasyukova EG,
816 Loeschcke V, Pascual M, Vieira CP, Serga S, Montchamp-Moreau C, Abbott J, Gibert P,

Porcelli D, Posnien N, Sánchez-Gracia A, Grath S, Sucena É, Bergland AO, Guerreiro MPG, Onder BS, Argyridou E, Guio L, Schou MF, Deplancke B, Vieira C, Ritchie MG, Zwaan BJ, Tauber E, Orengo DJ, Puerma E, Aguadé M, Schmidt P, Parsch J, Betancourt AJ, Flatt T, González J. 2020. Genomic Analysis of European *Drosophila melanogaster* Populations Reveals Longitudinal Structure, Continent-Wide Selection, and Previously Unknown DNA Viruses. *Mol Biol Evol* **37**:2661–2678. doi:10.1093/molbev/msaa120

Kapun M, Fabian DK, Goudet J, Flatt T. 2016. Genomic Evidence for Adaptive Inversion Clines in *Drosophila melanogaster*. *Mol Biol Evol* **33**:1317–1336. doi:10.1093/molbev/msw016

Kapun M, Flatt T. 2019. The adaptive significance of chromosomal inversion polymorphisms in *Drosophila melanogaster*. *Mol Ecol* **28**:1263–1282. doi:10.1111/mec.14871

Karasov T, Messer PW, Petrov DA. 2010. Evidence that adaptation in *Drosophila* is not limited by mutation at single sites. *PLoS Genet* **6**:e1000924. doi:10.1371/journal.pgen.1000924

Kellermann V, Overgaard J, Hoffmann AA, Fløjgaard C, Svenning J-C, Loeschcke V. 2012. Upper thermal limits of *Drosophila* are linked to species distributions and strongly constrained phylogenetically. *Proc Natl Acad Sci U S A* **109**:16228–16233. doi:10.1073/pnas.1207553109

Kim YB, Oh JH, McIver LJ, Rashkovetsky E, Michalak K, Garner HR, Kang L, Nevo E, Korol AB, Michalak P. 2014. Divergence of *Drosophila melanogaster* repeatomes in response to a sharp microclimate contrast in Evolution Canyon, Israel. *Proc Natl Acad Sci U S A* **111**:10630–10635. doi:10.1073/pnas.1410372111

Koboldt DC, Zhang Q, Larson DE, Shen D, McLellan MD, Lin L, Miller CA, Mardis ER, Ding L, Wilson RK. 2012. VarScan 2: somatic mutation and copy number alteration discovery in cancer by exome sequencing. *Genome Res* **22**:568–576. doi:10.1101/gr.129684.111

Kolaczkowski B, Kern AD, Holloway AK, Begun DJ. 2011. Genomic differentiation between temperate and tropical Australian populations of *Drosophila melanogaster*. *Genetics* **187**:245–260. doi:10.1534/genetics.110.123059

Korol AB, Kirzhner VM, Ronin YI, Nevo E. 1996. Cyclical environmental changes as a factor maintaining genetic polymorphism. 2. Diploid selection for an additive trait. *Evol Int J Org Evol* **50**:1432–1441. doi:10.1111/j.1558-5646.1996.tb03917.x

Kostál V. 2006. Eco-physiological phases of insect diapause. *J Insect Physiol* **52**:113–127. doi:10.1016/j.jinsphys.2005.09.008

Lack JB, Lange JD, Tang AD, Corbett-Detig RB, Pool JE. 2016. A Thousand Fly Genomes: An Expanded *Drosophila* Genome Nexus. *Mol Biol Evol* **33**:3308–3313. doi:10.1093/molbev/msw195

Lande R. 2008. Adaptive topography of fluctuating selection in a Mendelian population. *J Evol Biol* **21**:1096–1105. doi:10.1111/j.1420-9101.2008.01533.x

Levins RA. 1974. Evolution in changing environments ; some theoretical explorations, 3. printing. ed, Monographs in population biology. Princeton, NJ: Princeton Univ. Press.

Li H, Durbin R. 2009. Fast and accurate short read alignment with Burrows-Wheeler transform. *Bioinforma Oxf Engl* **25**:1754–1760. doi:10.1093/bioinformatics/btp324

Li H, Handsaker B, Wysoker A, Fennell T, Ruan J, Homer N, Marth G, Abecasis G, Durbin R, 1000 Genome Project Data Processing Subgroup. 2009. The Sequence Alignment/Map format and SAMtools. *Bioinforma Oxf Engl* **25**:2078–2079. doi:10.1093/bioinformatics/btp352

Lynch M, Ho W-C. 2020. The Limits to Estimating Population-Genetic Parameters with Temporal Data. *Genome Biol Evol* **12**:443–455. doi:10.1093/gbe/evaa056

Machado HE, Bergland AO, O'Brien KR, Behrman EL, Schmidt PS, Petrov DA. 2016. Comparative population genomics of latitudinal variation in *Drosophila simulans* and *Drosophila melanogaster*. *Mol Ecol* **25**:723–740. doi:https://doi.org/10.1111/mec.13446

Mackay TFC, Richards S, Stone EA, Barbadilla A, Ayroles JF, Zhu D, Casillas S, Han Y, Magwire MM, Cridland JM, Richardson MF, Anholt RRH, Barrón M, Bess C, Blankenburg KP, Carbone MA, Castellano D, Chaboub L, Duncan L, Harris Z, Javaid M, Jayaseelan JC, Jhangiani SN, Jordan KW, Lara F, Lawrence F, Lee SL, Librado P, Linheiro RS, Lyman RF, Mackey AJ, Munidasa M, Muzny DM, Nazareth L, Newsham I, Perales L, Pu L-L, Qu C, Ràmia M, Reid JG, Rollmann SM, Rozas J, Saada N, Turlapati L, Worley KC, Wu Y-Q, Yamamoto A, Zhu Y, Bergman CM, Thornton KR, Mittelman D, Gibbs RA. 2012. The *Drosophila melanogaster* Genetic Reference Panel. *Nature* **482**:173–178.

doi:10.1038/nature10811
MacMillan HA, Ferguson LV, Nicolai A, Donini A, Staples JF, Sinclair BJ. 2015. Parallel ionoregulatory adjustments underlie phenotypic plasticity and evolution of *Drosophila* cold tolerance. *J Exp Biol* **218**:423–432. doi:10.1242/jeb.115790
Mallard F, Nolte V, Tobler R, Kapun M, Schlötterer C. 2018. A simple genetic basis of adaptation to a novel thermal environment results in complex metabolic rewiring in *Drosophila*. *Genome Biol* **19**:119. doi:10.1186/s13059-018-1503-4
Martin M. 2011. Cutadapt removes adapter sequences from high-throughput sequencing reads. *EMBnet.journal* **17**:10–12. doi:10.14806/ej.17.1.200
McKenna A, Hanna M, Banks E, Sivachenko A, Cibulskis K, Kernytsky A, Garimella K, Altshuler D, Gabriel S, Daly M, DePristo MA. 2010. The Genome Analysis Toolkit: a MapReduce framework for analyzing next-generation DNA sequencing data. *Genome Res* **20**:1297–1303. doi:10.1101/gr.107524.110
Menne MJ, Durre I, Vose RS, Gleason BE, Houston TG. 2012. An Overview of the Global Historical Climatology Network-Daily Database. *J Atmospheric Ocean Technol* **29**:897–910. doi:10.1175/JTECH-D-11-00103.1
Nosil P, Villoutreix R, de Carvalho CF, Feder JL, Parchman TL, Gompert Z. 2020. Ecology shapes epistasis in a genotype-phenotype-fitness map for stick insect colour. *Nat Ecol Evol* **4**:1673–1684. doi:10.1038/s41559-020-01305-y
Overgaard J, Kristensen TN, Mitchell KA, Hoffmann AA. 2011. Thermal tolerance in widespread and tropical *Drosophila* species: does phenotypic plasticity increase with latitude? *Am Nat* **178 Suppl 1**:S80-96. doi:10.1086/661780
Overgaard J, MacMillan HA. 2017. The Integrative Physiology of Insect Chill Tolerance. *Annu Rev Physiol* **79**:187–208. doi:10.1146/annurev-physiol-022516-034142
Paaby AB, Bergland AO, Behrman EL, Schmidt PS. 2014. A highly pleiotropic amino acid polymorphism in the *Drosophila* insulin receptor contributes to life-history adaptation. *Evol Int J Org Evol* **68**:3395–3409. doi:10.1111/evo.12546
Pool JE, Corbett-Detig RB, Sugino RP, Stevens KA, Cardeno CM, Crepeau MW, Duchen P, Emerson JJ, Saelao P, Begun DJ, Langley CH. 2012. Population Genomics of sub-saharan *Drosophila melanogaster*: African diversity and non-African admixture. *PLoS Genet* **8**:e1003080. doi:10.1371/journal.pgen.1003080
Rajpurohit S, Gefen E, Bergland AO, Petrov DA, Gibbs AG, Schmidt PS. 2018. Spatiotemporal dynamics and genome-wide association analysis of desiccation tolerance in *Drosophila melanogaster*. *Mol Ecol* **27**:3525–3540. doi:10.1111/mec.14814
Rajpurohit S, Hanus R, Vrkoslav V, Behrman EL, Bergland AO, Petrov D, Cvačka J, Schmidt PS. 2017. Adaptive dynamics of cuticular hydrocarbons in *Drosophila*. *J Evol Biol* **30**:66–80. doi:10.1111/jeb.12988
Reinhardt JA, Kolaczkowski B, Jones CD, Begun DJ, Kern AD. 2014. Parallel geographic variation in *Drosophila melanogaster*. *Genetics* **197**:361–373. doi:10.1534/genetics.114.161463
Rodríguez-Trelles F, Tarrío R, Santos M. 2013. Genome-wide evolutionary response to a heat wave in *Drosophila*. *Biol Lett* **9**:20130228. doi:10.1098/rsbl.2013.0228
Rudman SM, Barbour MA, Csilléry K, Gienapp P, Guillaume F, Hairston NG, Hendry AP, Lasky JR, Rafajlović M, Räsänen K, Schmidt PS, Seehausen O, Therkildsen NO, Turcotte MM, Levine JM. 2018. What genomic data can reveal about eco-evolutionary dynamics. *Nat Ecol Evol* **2**:9–15. doi:10.1038/s41559-017-0385-2
Rudman SM, Greenblum S, Hughes RC, Rajpurohit S, Kiratli O, Lowder DB, Lemmon SG, Petrov DA, Chaston JM, Schmidt P. 2019. Microbiome composition shapes rapid genomic adaptation of *Drosophila melanogaster*. *Proc Natl Acad Sci* **116**:20025–20032. doi:10.1073/pnas.1907787116
Samuk K, Owens GL, Delmore KE, Miller SE, Rennison DJ, Schluter D. 2017. Gene flow and selection interact to promote adaptive divergence in regions of low recombination. *Mol Ecol* **26**:4378–4390. doi:https://doi.org/10.1111/mec.14226
Scheiner SM. 1993. Genetics and Evolution of Phenotypic Plasticity. *Annu Rev Ecol Syst* **24**:35–68. doi:10.1146/annurev.es.24.110193.000343
Schlötterer C, Tobler R, Kofler R, Nolte V. 2014. Sequencing pools of individuals - mining genome-

927 wide polymorphism data without big funding. *Nat Rev Genet* **15**:749–763.
928 doi:10.1038/nrg3803
929 Schmidt PS, Conde DR. 2006. Environmental heterogeneity and the maintenance of genetic variation
930 for reproductive diapause in *Drosophila melanogaster*. *Evol Int J Org Evol* **60**:1602–1611.
931 Schoener TW. 2011. The Newest Synthesis: Understanding the Interplay of Evolutionary and
932 Ecological Dynamics. *Science* **331**:426–429. doi:10.1126/science.1193954
933 Shpak M, Wakeley J, Garrigan D, Lewontin RC. 2010. A structured coalescent process for seasonally
934 fluctuating populations. *Evol Int J Org Evol* **64**:1395–1409. doi:10.1111/j.1558-
935 5646.2009.00891.x
936 Siepielski AM, DiBattista JD, Carlson SM. 2009. It's about time: the temporal dynamics of
937 phenotypic selection in the wild. *Ecol Lett* **12**:1261–1276. doi:https://doi.org/10.1111/j.1461-
938 0248.2009.01381.x
939 Signor S. 2017. Population genomics of Wolbachia and mtDNA in *Drosophila simulans* from
940 California. *Sci Rep* **7**:13369. doi:10.1038/s41598-017-13901-3
941 Stalker HD. 1980. Chromosome Studies in Wild Populations of *Drosophila melanogaster*. II.
942 Relationship of Inversion Frequencies to Latitude, Season, Wing-Loading and Flight Activity.
943 *Genetics* **95**:211–223.
944 Stalker HD. 1976. Chromosome studies in wild populations of *D. melanogaster*. *Genetics* **82**:323–
945 347.
946 Svetec N, Cridland JM, Zhao L, Begun DJ. 2016. The Adaptive Significance of Natural Genetic
947 Variation in the DNA Damage Response of *Drosophila melanogaster*. *PLoS Genet*
948 **12**:e1005869. doi:10.1371/journal.pgen.1005869
949 Tauber MJ, Tauber CA, Masaki S. 1986. Seasonal adaptations of insects. New York: Oxford
950 University Press.
951 Thompson JN. 1998. Rapid evolution as an ecological process. *Trends Ecol Evol* **13**:329–332.
952 doi:10.1016/S0169-5347(98)01378-0
953 Tobler R, Franssen SU, Kofler R, Orozco-Terwengel P, Nolte V, Hermisson J, Schlötterer C. 2014.
954 Massive habitat-specific genomic response in *D. melanogaster* populations during
955 experimental evolution in hot and cold environments. *Mol Biol Evol* **31**:364–375.
956 doi:10.1093/molbev/mst205
957 Tuttle EM, Bergland AO, Korody ML, Brewer MS, Newhouse DJ, Minx P, Stager M, Betuel A,
958 Cheviron ZA, Warren WC, Gonser RA, Balakrishnan CN. 2016. Divergence and Functional
959 Degradation of a Sex Chromosome-like Supergene. *Curr Biol* **26**:344–350.
960 doi:10.1016/j.cub.2015.11.069
961 van Heerwaarden B, Hoffmann AA. 2007. Global Warming: Fly Populations Are Responding
962 Rapidly to Climate Change. *Curr Biol* **17**:R16–R18. doi:10.1016/j.cub.2006.11.035
963 Via S, Lande R. 1985. Genotype-Environment Interaction and the Evolution of Phenotypic Plasticity.
964 *Evolution* **39**:505. doi:10.2307/2408649
965 Wiman NG, Walton VM, Dalton DT, Anfora G, Burrack HJ, Chiu JC, Daane KM, Grassi A, Miller B,
966 Tochen S, Wang X, Ioriatti C. 2014. Integrating Temperature-Dependent Life Table Data into
967 a Matrix Projection Model for *Drosophila* suzukii Population Estimation. *PLoS ONE*
968 **9**:e106909. doi:10.1371/journal.pone.0106909
969 Wittmann MJ, Bergland AO, Feldman MW, Schmidt PS, Petrov DA. 2017. Seasonally fluctuating
970 selection can maintain polymorphism at many loci via segregation lift. *Proc Natl Acad Sci*
971 **114**:E9932–E9941. doi:10.1073/pnas.1702994114
972 Yoshida T, Jones LE, Ellner SP, Fussmann GF, Hairston NG. 2003. Rapid evolution drives ecological
973 dynamics in a predator–prey system. *Nature* **424**:303–306. doi:10.1038/nature01767
974 Zhao L, Begun DJ. 2017. Genomics of parallel adaptation at two timescales in *Drosophila*. *PLoS*
975 *Genet* **13**:e1007016. doi:10.1371/journal.pgen.1007016
976 Zhu Y, Bergland AO, González J, Petrov DA. 2012. Empirical validation of pooled whole genome
977 population re-sequencing in *Drosophila melanogaster*. *PloS One* **7**:e41901.
978 doi:10.1371/journal.pone.0041901
979

Supplemental Information

Supplemental Table 1: Population information with sampling meta-data

Supplemental Table 2: Top 1% of seasonal SNPs (regression beta and p-values) based on GLM model. Coordinates are in *D. melanogaster* reference v5.5.

Supplemental Figure 1. Extended sampling figure.

Supplemental Figure 2. Site frequency spectrum.

Supplemental Figure 3. Chromosome level enrichment tests.

Supplemental Figure 4. Bayenv seasonal analysis.

Supplemental Figure 5. Comparison of the GLM and the Bayenv model for assessing clinal and seasonal concordance.

Supplemental Figure 6. Inversion frequencies.

Supplemental Figure 7. Simulation of competitive mapping to evaluation *D. simulans* contamination.

Supplemental Figure 8. The effect of artificial increases of sample size on model output.

980

Supplemental Figure 1

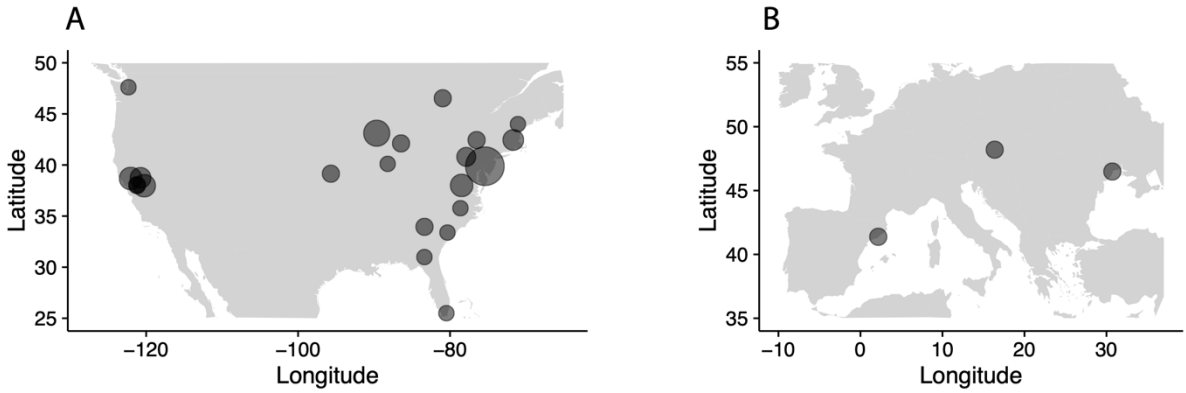

Supplemental Figure 1. Sampling localities in A) North America and B) Europe for all samples collected, regardless of use in the present analysis. Sizes of circles reflect number of samples per locality.

Supplemental Figure 2

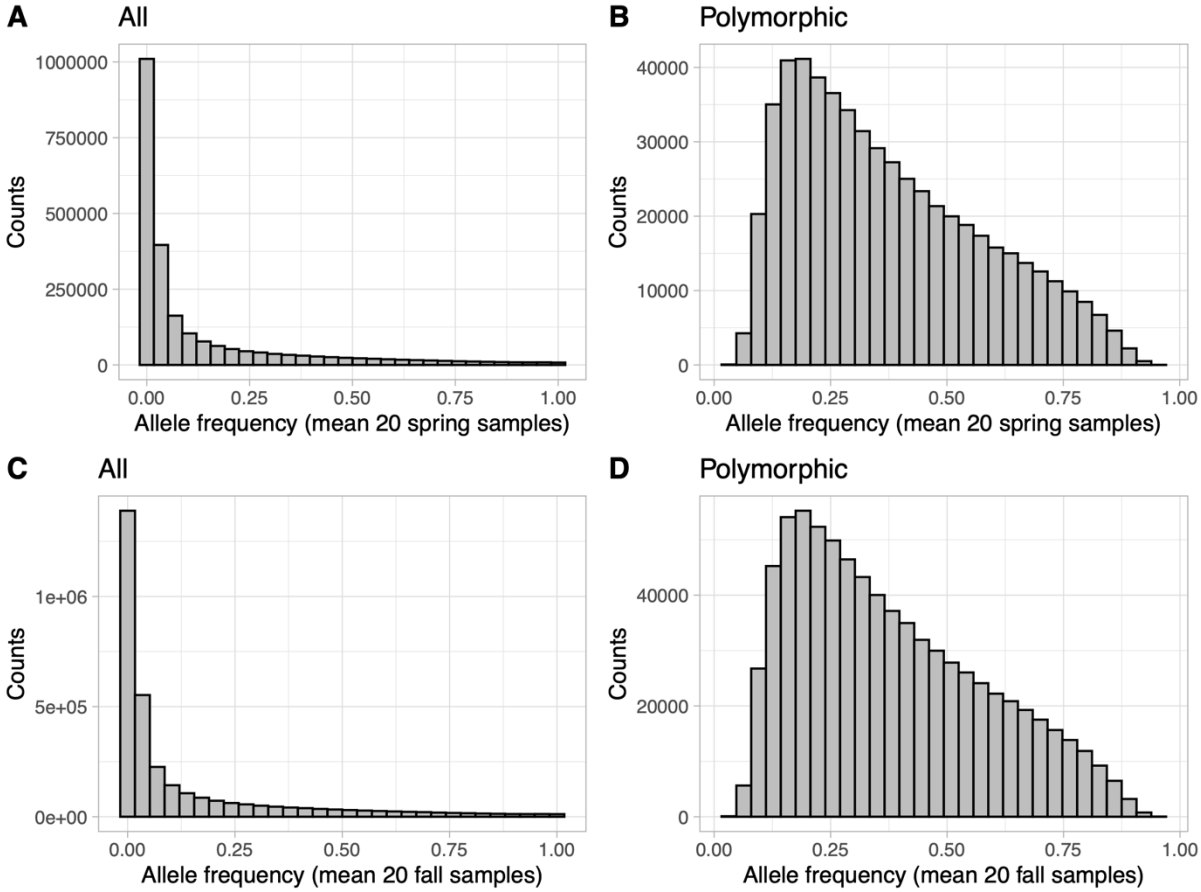

Supplemental Figure 2. Distributions of the mean spring (A/B) and mean fall (C/D) allele frequencies for the dataset before (A/C) and after (B/D) filtering SNP found to be monomorphic in any population.

982

Supplemental Figure 3

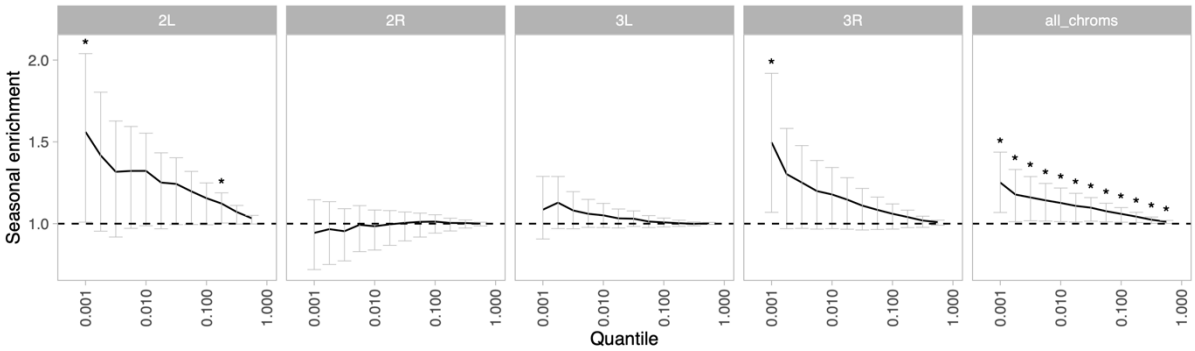

Supplemental Figure 3. Enrichment of seasonal SNPs (median of 500 permutations) by chromosome and significance threshold. Enrichment is calculated as the observed number of seasonal SNPs over the number of seasonal SNPs in each permutation. Error bars are 95% confidence intervals and asterisks denote greater seasonal enrichment than more than 95% of permutations.

989
990 **Supplemental Figure 4**

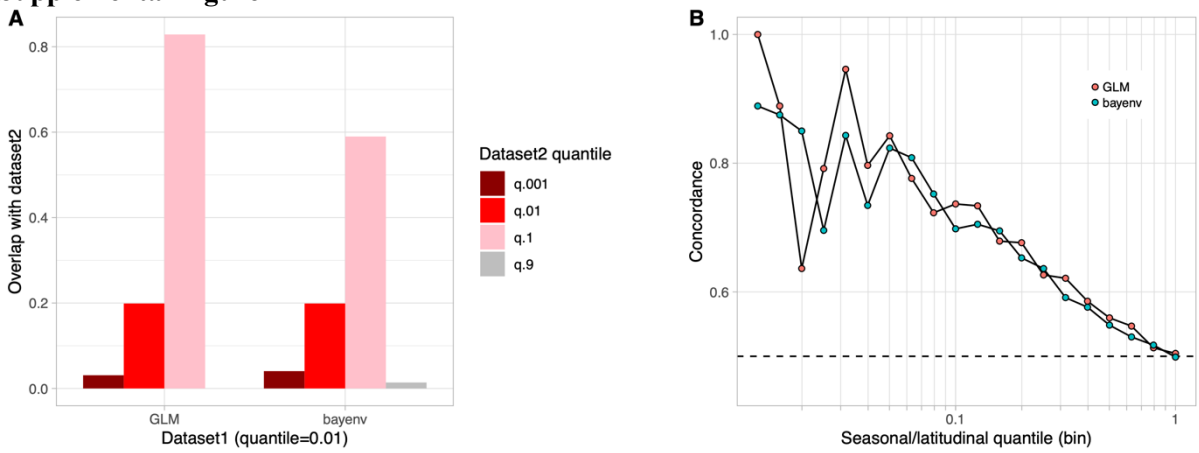

991
992
993

Supplemental Figure 4. Bayenv seasonal analysis. A) Proportion of SNPs found highly seasonal in both the GLM and the bayenv seasonal analyses. B) Seasonal and latitudinal concordance for both the GLM and the bayenv analyses.

994

Supplemental Figure 5

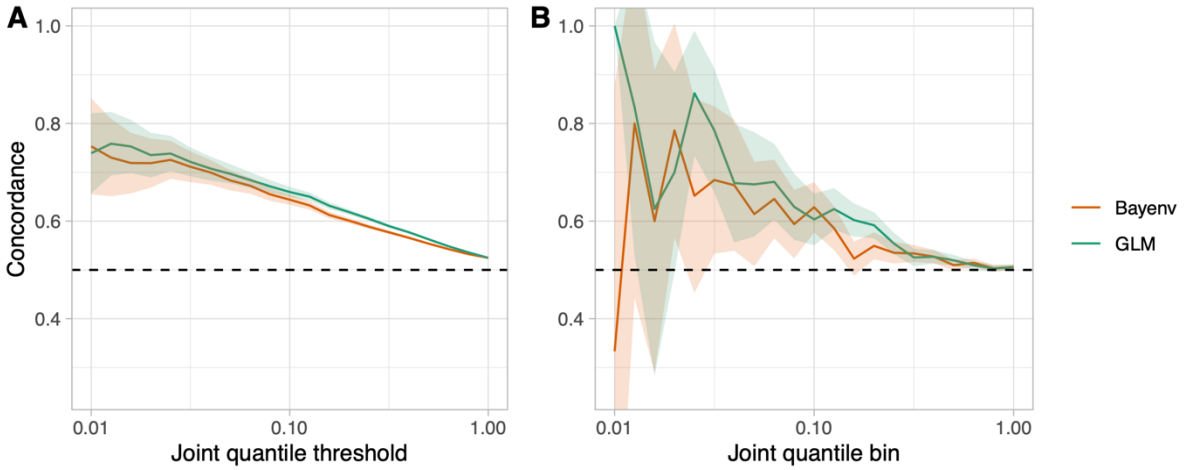

Supplemental Figure 5. Comparison of the GLM and the Bayenv model for assessing clinal and seasonal concordance. A) The "joint quantile threshold" is the quantile threshold for both the seasonal and the clinal analysis, and includes all SNPs at that quantile or less. B) The "joint quantile bin" includes only those SNPs at that specific quantile.

Supplemental Figure 6

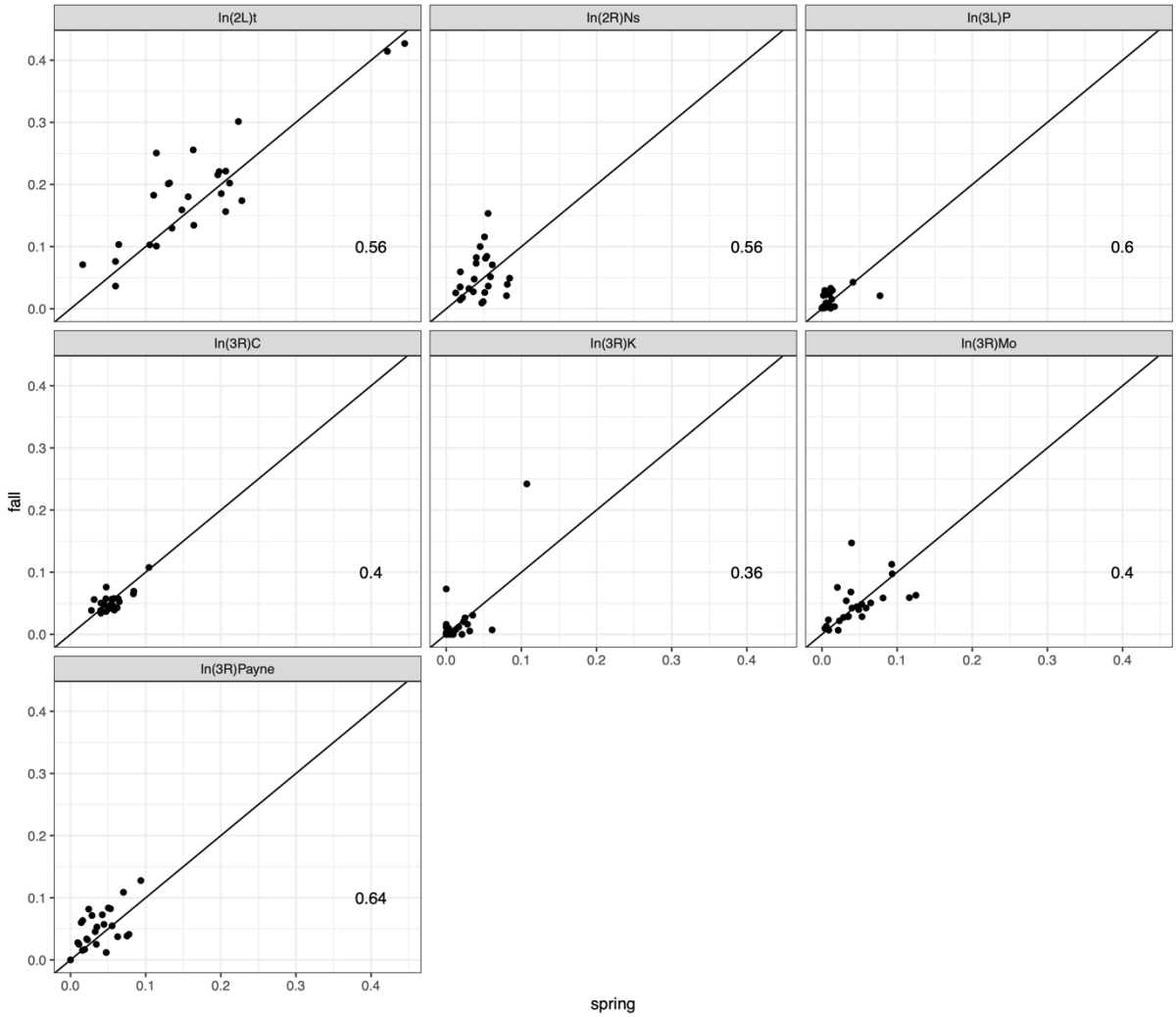

Supplemental Figure 6. Inversion frequencies. Each datapoint is a separate population. Numbers are the fraction of populations where spring is greater than fall.

1002 **Supplemental Figure 7**
1003

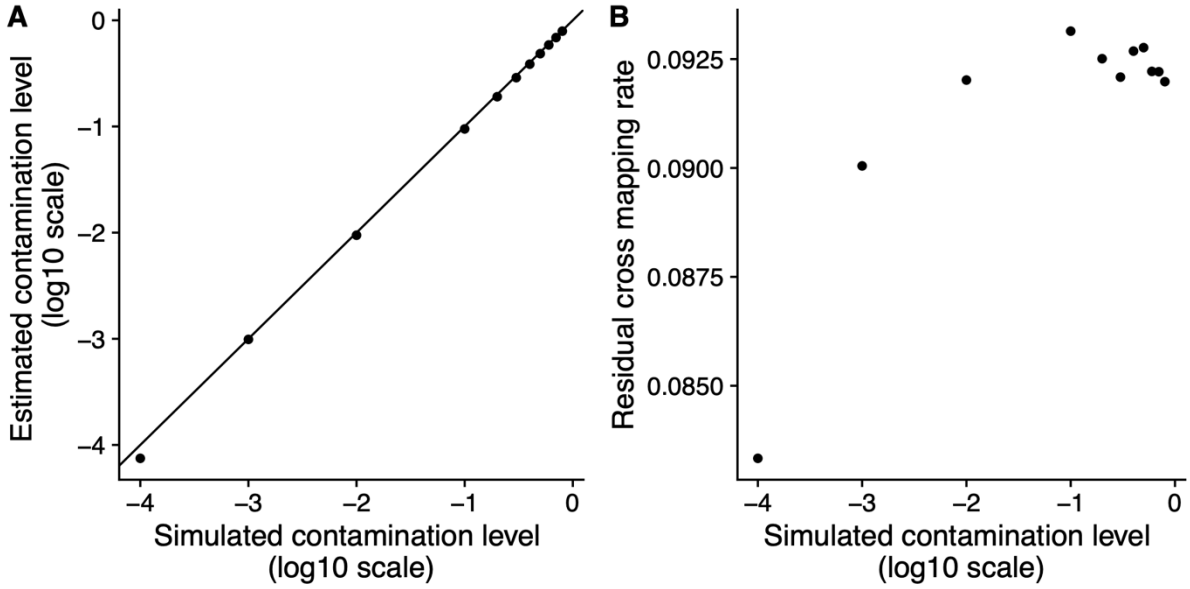

1004
1005

Supplemental Figure 7. Competitive mapping effectively reduces cross species mapping between *D. simulans* and *D. melanogaster*. (A) The estimated rate of *D. simulans* contamination can be precisely estimated by calculating the number of reads mapping preferentially to the *D. simulans* genome. Estimated contamination rates are ~2% lower than the expected rate. (B) The residual cross species mapping rate, i.e. the fraction of *D. simulans* reads mapping to the *D. melanogaster* genome is roughly consistent at ~9%.

1006
1007

1008 **Supplemental Figure 8**

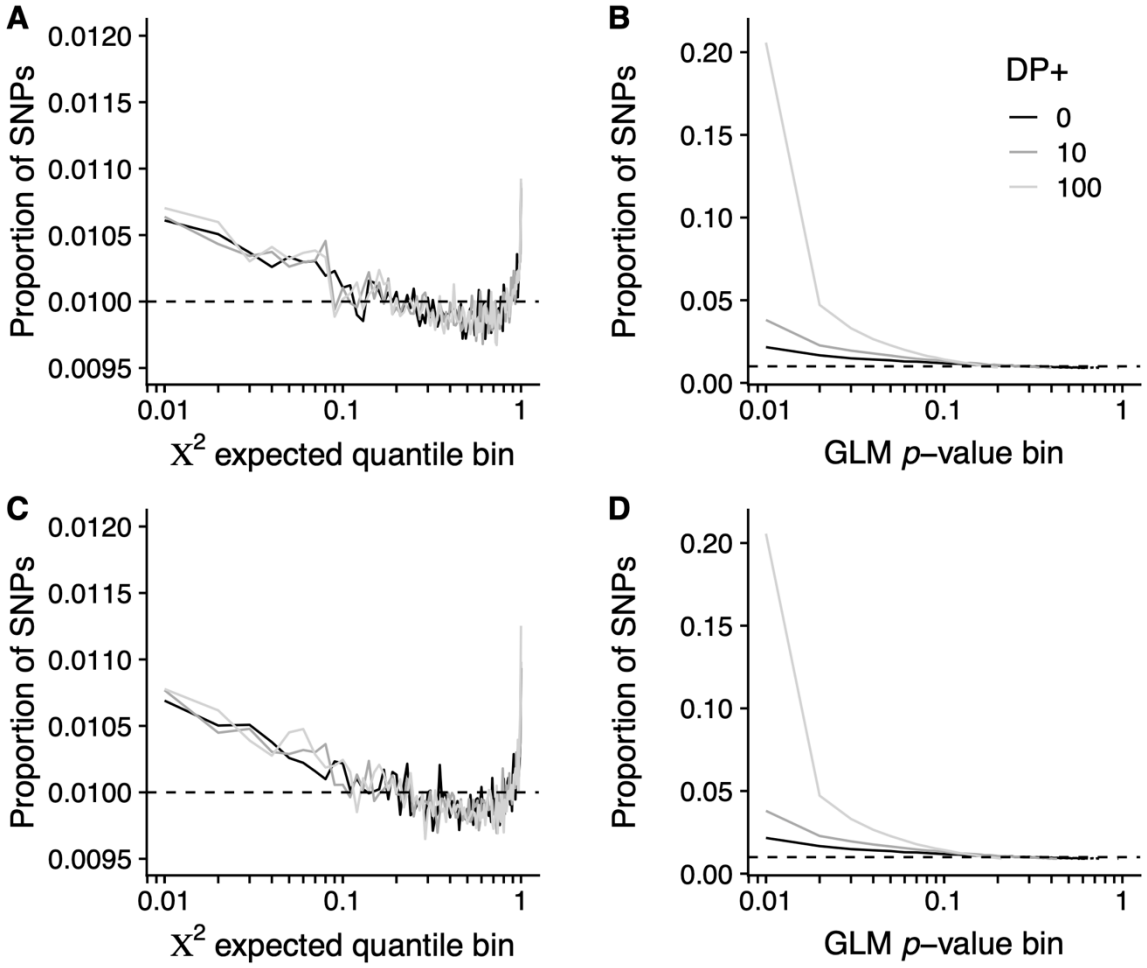

1009
1010

Supplemental Figure 8. The effect of artificial increases of sample size on the Core20 seasonal analysis using A,C) the RFM and B,D) the GLM analyses. Top row: sample size inflated by a fixed amount. Bottom row: sample size inflated by a Poisson sampled amount. Shown is the proportion of SNPs in each bin (solid lines) compared with the null expectation (dashed line). Black: original dataset. Dark grey: 10 reads added to each sample (same allele frequencies). Light grey: 100 reads added to each sample (same allele frequencies).